Cerna, Fernando V.; Pourakbari-Kasmaei, Mahdi; Barros, Raone G.; Naderi, Ehsan; Lehtonen, Matti; Contreras, Javier

Optimal operating scheme of neighborhood energy storage communities to improve power grid performance in smart cities

Published in:
Applied Energy

DOI:
10.1016/j.apenergy.2022.120411

Published: 01/02/2023

Document Version
Peer-reviewed accepted author manuscript, also known as Final accepted manuscript or Post-print

Optimal Operating Scheme of Neighborhood Energy Storage Communities to Improve Power Grid Performance in Smart Cities

Fernando V. Cerna[1,2 *], Mahdi Pourakbari-Kasmaei[3], Raone G. Barros[1], Ehsan Naderi[4], Matti Lehtonen[3], Javier Contreras[5]

[1] Department of Electrical Engineering, Federal University of Roraima, Boa Vista 69310-000, Brazil.

[2] Postgraduate Program in Natural Resources, Research Area in Management and Dynamics of Natural Resources – Renewable Energies, Federal University of Roraima, Av. Nova Iorque – Aeroporto, Boa Vista 69310-000, Brazil.

[3] Department of Electrical Engineering and Automation, Aalto University, 02150 Espoo, Finland.

[4] School of Electrical, Computer, and Biomedical Engineering, Southern Illinois University, Carbondale, IL 62901, USA.

[5] School of Industrial Engineering, University of Castilla-La Mancha, 13071 Ciudad Real, Spain.

[*]Corresponding author.

E-mail addresses: Fernando.Cerna@ufrr.br, Mahdi.Pourakbari@aalto.fi, Raone.Barros@ufrr.br, Ehsan.Naderi@siu.edu, Matti.Lehtonen@aalto.fi, Javier.Contreras@uclm.es.

Abstract: In *Smart Cities* (SC), the efficient management of services such as health, transport, public safety, and especially the electricity ensures the welfare of citizens. In recent years, the insertion of renewable sources (RSs) (e.g., solar and wind) in the power grid (PG) of SCs has contributed to meeting the electricity needs of the various consumer units. However, the large-scale integration of these RSs can fatigue the assets, leading to their premature aging and, consequently, compromising the quality of electricity supply. To overcome these challenges, the implementation of Neighboring Energy Storage Communities (NESCs) employing demand response (DR) strategies along with efficient coordination of storage batteries (SBs) could be a promising alternative. In this sense, the present work proposes a mixed-integer linear programming (MILP) model to efficiently manage SBs and the set of household appliances, including charging electric vehicles (EVs), in an NESC provided solely by PG. The proposed model aims to minimize: the total costs related to energy consumption, the peak rebound effect on the total consumption profile, energy wastage through load factor (LF) improvement, and the deep discharges in the SBs during their daily operational cycle. Operational constraints related to the home appliances, such as average usage time, the number of times that the appliance is used daily, etc., are taking into account. The EV state-of-charge (SOC), EV charging rate limits, and initial and final SOC of the SBs, are also considered. A Monte Carlo Algorithm (MCA) is used

to simulate the habitual consumption patterns of each customer. The proposed model was implemented in AMPL and solved using CPLEX. The performance of this proposed model is evaluated considering two NESCs differentiated by the number of consumer communities. A first NESC (small-scale) is analyzed considering only two consumer communities. In this NESC, two case studies (Case 1 and 2) are discussed. Next, the second NESC (large-scale) that considers 14 consumer communities is analyzed for the most complete case study (Case 2). Within each NESC, consumer communities are differentiated by the household income and the types of SBs (individual and shared) that support each community. The results corroborate the applicability of the MILP model to real case studies on a diverse scale, guaranteeing the efficient use of PG at the same time that each SB seeks the most optimized operation.

Keywords: Demand response, home appliances, mixed-integer linear programming, neighborhood energy storage communities, storage batteries, smart cities.

NOMENCLATURE

A. Abbreviation list

DISCOs	Distribution companies.
DR	Demand response
EVs	Electric vehicles
LF	Load factor
MILP	Mixed-integer linear programming
NESCs	Neighboring energy storage communities
PG	Power grid
RSs	Renewable sources
SBs	Storage batteries
SC	Smart cities
SOC	State of charge

B. Functions

$\mathcal{F}_1, \mathcal{F}_2, \mathcal{F}_3, \mathcal{F}_4$	Functions related to customers' energy bills, coincident usage of appliances, energy waste in the PG, and lifetime of SBs.
$\lvert . \rvert$	Cardinal of a set

C. Sets and indexes

u, a, t, b	Index for customers, home appliances, periods, and discrete blocks.
$\mathcal{U}^{c1}, \mathcal{U}^{c2}$	Set of consumers present in *Community 1* and *Community 2*.
$\mathcal{A}, \mathcal{T}, \mathcal{B}$	Sets related to the household appliances *a*, periods *t*, and discrete blocks *b*.

D. Parameters

General parameters

λ_t	Hourly tariff ($/kWh).
ϕ_a	Indicates the type of appliances *a* (-1: EV; 0: appliances with working hours less than 1 h; 1: appliances with working hours greater than or equal to 1 h).
β'_a	Binary parameter that adopts a value of 1 for higher average power appliances; otherwise, 0.
$ac, \mathcal{I}$	Accumulator and big value used in the linearization process.
P_a, P^e	Average power of appliance *a* and charging rate of the EV battery (kW).
Q_a	Number of times that appliance *a* is turned-on for less than 1 h.
$\underline{Q}_a / \overline{Q}_a$	Min. and max. number of times that appliance *a* is turned on throughout the day.
Ti_a^{av}	Average time that appliance *a* is turned-on for consumption (h).
$[\underline{Ti}_a, \overline{Ti}_a]$	Time interval within the period *t* in which appliance *a* is turned-on (h).
Δt	Duration of each period *t* (h).
$\mathrm{X}_{t,b}$	Inclination value related to discrete block *b* in period *t*.
$\overline{\Delta}_t$	Upper limit related to variable $\Delta \mathrm{Y}_{t,b}$.
$\Theta_{a,t}, \widehat{\Theta}_{a,t}$	Probability distribution/accumulated probability distribution related to the consumption of household appliances *a* in period *t*.
$\rho_1, \rho_2, \rho_3, \rho_4$	Weights related to $\mathcal{F}_1$, $\mathcal{F}_2$, $\mathcal{F}_3$, and $\mathcal{F}_4$.

Parameters related to Community 1

$\mathcal{C}_{u,a,t}^{c1}$	Habitual consumption profile. Indicates the energy consumed by customer *u* when turning-on appliance *a* in period *t* (kWh).
$\mathcal{W}_{u,a,t}^{c1}$	Binary value that indicates the status of a given appliance *a* (1: customer *u* has turned-on appliance *a* in period *t*; 0: otherwise).
$\mathcal{B}^{c1}$	Shared SB capacity (kWh).
$\mathcal{E}^{o\_c1}$	Initial SOC of the shared SB (kWh).
$\underline{\gamma}^{c1} / \overline{\gamma}^{c1}$	Percentage values related to $\mathcal{B}^{c1}$. Thus, $\underline{\gamma}^{c1} \times \mathcal{B}^{c1}$ indicates the minimum discharging limit for SB, and $\overline{\gamma}^{c1} \times \mathcal{B}^{c1}$ is the maximum charging limit for this SB.
$\eta^{inj\_c1} / \eta^{abs\_c1}$	Shared SB injection/absorption efficiency.
$\underline{P}^{inj\_c1} / \overline{P}^{inj\_c1}$	Min. / max. limits of the power injected by shared SB (kW).
$\underline{P}^{abs\_c1} / \overline{P}^{abs\_c1}$	Min. / max. limits of the power absorbed by shared SB (kW).

Parameters related to Community 2

$\mathcal{C}_{u,a,t}^{c2}$	Habitual consumption profile. Indicates the energy consumed by customer *u* when turning-on appliance *a* in period *t* (kWh).
$\mathcal{C}_t^{c2}, \mathcal{C}^{c2,max}$	Habitual energy consumption in each period *t* during the day obtained from $\mathcal{C}_{u,a,t}^{c2}$, and maximum value of $\mathcal{C}_t^{c2}$ (kWh).
$\mathcal{W}_{u,a,t}^{c2}$	Binary value that indicates the status of a given appliance *a* (1: customer *u* has turned on appliance *a* in period *t*; 0: otherwise).
BEV_u	EV battery capacity (kWh).
$\underline{Q}_u^c / \overline{Q}_u^c$	Min. and max. number of times that the EV battery related to customer *u* can be charged.
SOC_u^0	Initial SOC of the EV battery related to user *u* (kWh).
$\beta''_{u,a,t}$	Customer hourly preference. Indicates the period(s) *t* in which appliance *a* can be connected for consumption without affecting customer *u* comfort.
$\left[\underline{Ti}_u^e, \overline{Ti}_u^e\right]$	Time variation interval of variable $Ti_{u,t}^e$ (h).
ξ	Percentage value related to BEV_u.
$\underline{\gamma}_u^{c2} / \overline{\gamma}_u^{c2}$	Percentage values related to $\mathcal{B}_u^{c2}$. Thus, $\underline{\gamma}_u^{c2} \times \mathcal{B}_u^{c2}$ indicates the minimum discharge limit of the SB *u*, and $\overline{\gamma}_u^{c2} \times \mathcal{B}_u^{c2}$ is the maximum charging limit of this SB.
$\mathcal{B}_u^{c2}$	SB capacity related to customer *u* (kWh).
$\mathcal{E}_u^{o\_c2}$	Initial SOC of the SB related to customer *u* (kWh).
$\eta_u^{inj\_c2} / \eta_u^{abs\_c2}$	SB *u* injection/absorption efficiency.
$\underline{P}_u^{inj\_c2} / \overline{P}_u^{inj\_c2}$	Min. / max. limits of the power injected by SB *u* (kW).
$\underline{P}_u^{abs\_c2} / \overline{P}_u^{abs\_c2}$	Min. / max. limits of the power absorbed by SB *u* (kW).

E. Variables

General variables

$P_t^{eg}, \tilde{P}^{eg}$	Continuous variable that represents the power supplied by PG in each period *t* and average value related to P_t^{eg} (kW).
Y_t	Represents the difference between P_t^{eg} and $\tilde{P}^{eg}$ in period *t*.
$\Delta\mathrm{Y}_{t,b} / \mathrm{Y}_t^+ / \mathrm{Y}_t^-$	Auxiliary variable to be used in the discretization process.

Variables related to Community 1

$P_t^{eg\_c1}$	Component of P_t^{eg} related to *Community 1* (kW). Indicates the power required/supplied by this community.
$P_{u,t}^{s\_c1}$	Power supplied for each customer's home *u* in each period *t* (kW).
$P_t^{inj\_c1} / P_t^{abs\_c1}$	Power injected/absorbed by the shared SB in each period *t* (kW).

$\alpha_t^{inj\_c1}/\alpha_t^{abs\_c1}$	Binary variables that indicate, for each period *t*, the power injection/absorption status of the shared SB.
$\mathcal{E}_t^{c1}$	SOC of the shared SB in each period *t* (kWh).

Variables related to Community 2

$\mathcal{W}_{u,a,t}^{ou}$	Binary value related to $\mathcal{O}_{u,a,t}$. Indicates the status of a given appliance *a* (1: customer *u* has connected the appliance *a* at period *t*; 0: otherwise).
$\mathcal{O}_{u,a,t}^{c2}$	Optimal consumption profile. Indicates the energy to be consumed by customer *u* when turning on appliance *a* in period *t* (kWh).
$\theta'_{u,t}$	Coincidence factor. Represents, for each customer *u*, the number of appliances that are turned on for consumption in the same period *t*.
$Ti_{u,a,t}^{on}$	Continuous variable that represents for each customer *u* the time that appliance *a* is turned on in period *t* (h).
$\mathcal{G}_{u,t}^{ev}$	Continuous variable that represents, for each customer *u*, the SOC in the EV battery in period *t* (kWh).
$Ti_{u,t}^{e}$	Continuous variable that represents the charging time of the EV battery in period *t* for customer *u* (h).
$\mathcal{G}_u^s$	Continuous variable that represents the total SOC of the EV battery for each customer *u* (kWh).
$\Delta Ti_{u,a,t}^{on}, \Delta Ti_{u,a,t}^{e}$	Represent the product $\mathcal{W}_{u,a,t}^{ou} \times Ti_{u,a,t}^{on}$ and $\mathcal{W}_{u,a,t}^{ou} \times Ti_{u,a,t}^{e}$ to be linearized.
$P_t^{eg\_c2}$	Component of P_t^{eg} related to *Community 2* (kW). Indicates the power required/supplied by this community.
$P_{u,t}^{s\_c2}$	Power provided to SB and home related to customer *u* in period *t* (kW).
$P_{u,t}^{h}$	Power supplied for each customer's home *u* in period *t* (kW).
$P_{u,t}^{inj\_c2}/P_{u,t}^{abs\_c2}$	Power injected/absorbed by SB *u* in period *t* (kW).
$\alpha_{u,t}^{inj\_c2}/\alpha_{u,t}^{abs\_c2}$	Binary variable that indicates for each period *t* the power injection/absorption status of SB *u*.
$\mathcal{E}_{u,t}^{c2}$	SOC of customer's SB *u* in period *t* (kWh).

1. INTRODUCTION

1.1. Context

By 2050, the population in the world's cities will double at a rate of 60 million citizens per year [1]. In this possible context, services such as electricity, transport, health, education, etc., will experience high demand, thus compromising their quality [2]. Given this situation, the concept of *Smart Cities* (SC) has emerged in recent decades as an efficient way to manage these services, ensuring the social welfare of the inhabitants [3].

Among these essential services, the management of electricity consumption plays a vital role in meeting the needs of various consumption units, such as residential, commercial, industrial, and public lighting, to mention a few [4, 5]. With the integration of renewable sources (RSs), e.g., solar and wind, in the energy matrix of the SCs, distribution companies (DISCOs) and customers obtain financial and operational gains, such as reduction in energy bills and sale of surplus energy produced, and savings in investments related to maintenance and expansion of PG [6, 7, 8]. However, when the integration of these RSs takes place on a large scale, the power supply network can present several disturbances, among them, the congestion of the feeders leading to voltage fluctuations in the PG [9]. Consequently, the main assets, such as feeders, transformers, circuit breakers, etc., can reach premature aging, harming the performance of the PG as a whole [10].

A promising alternative to address these concerns is the efficient coordination between demand response (DR) strategies and the operation of storage batteries (SBs) in consumer communities supplied only by PG. In this work, these communities are called Neighboring Energy Storage Communities (NESCs). Thus, NESCs can schedule the usage of their home appliances and charging of their electric vehicles (EVs) through DR strategies, while SBs allow managing the energy provided by the PG [11, 12]. By employing price-based DR strategies, e.g., Time-of-Use (TOU), Critical Peak Pricing (CPP), Real-Time Pricing (RTP), etc. [13], NESCs will be able to reduce or shift the demand to times of day with lower energy rates [14]. In addition, to avoid the appearance of new peaks (the well-known peak rebound) at these times of the day (off-peak periods), improving the load factor (LF) can be used to enhance the DR strategy [15]. The LF is calculated as the average demand divided by the maximum demand for a given period (day, week, month, etc.) and varies between 0 and 1. When LF adopts 1, the energy consumption during the day has a wide distribution, indicating efficient use of electricity; otherwise, when LF is close to 0, the consumption profile presents several peaks, and this value indicates energy wastage [16].

Along with the DR strategy, the efficient operation of SBs within NESCs will allow energy to be stored (according to their capacity) based on the tariff scheme and consumption level of each customer. In this way, at times of day that present a cheaper tariff and reduced energy consumption, the SBs can store part of the energy coming from the PG [17]. Complementarily, at times of expensive tariffs and with greater consumption of electricity by NESCs, the energy previously stored in the SBs can be used to supply part of this consumption [18]. Thus, NESCs show their potential to efficiently manage the energy supplied by PG while representing an economical option to meet the electricity consumption of consumer communities without the need to increase RSs in the supply network.

As mentioned above, the excessive dissemination of RSs in SC can compromise the performance of its PG. In this sense, the search for power supply schemes based on SBs and DR programs as an alternative to alleviate the high use of RSs is an operational need that must be

met. To this end, efficient computational tools must be developed to support the decision-making of DISCOs and customers. Therefore, these aspects represent our main motivation for the development of the present work.

1.2. Related works

In the literature review, the works related to energy management schemes in consumer communities can be classified in three directions. The first one aims to maximize consumer financial gains by selling surplus energy produced/stored by RSs/SBs. In [19], an efficient control strategy of RSs and SBs was performed using game theory, allowing communities to maximize their surplus energy sales to DISCO. The authors in [20] proposed an efficient scheme for producing solar energy in consumer communities. This scheme aimed to optimize self-consumption in communities and reduce losses in the supply network. Similarly, the authors in [11] developed a strategy to reduce the daily consumption of electricity in communities through the optimal management of the renewable energy produced. This strategy considered the consumption preferences of customers in each community. In addition, a methodology was implemented in [12] to minimize operating expenses in communities. The expenses covered the sharing of surplus energy produced by solar sources present in the communities. In order to save on electricity bills for consumers, the researchers in [21] developed an efficient control strategy for RSs to support energy generation through fuel cells in consumer communities in Egypt. This strategy aimed to maximize the surplus energy produced to be injected into the PG. Using a neural network to predict the production of surplus power in customer communities, the work in [22] developed a methodology to optimize the sale of this surplus power with other communities and PG. Another energy trading scheme related to the production of RSs in communities was developed by [23]. In this work, the SBs were used as a support to manage the production of surpluses to maximize the financial gains of consumers.

The second direction involves works related to the sizing and operation of SBs in communities with RSs. For example, in [10], a predictive control scheme for SBs was implemented to support solar rooftops in consumer communities. Meteorological information and consumption patterns of each customer are part of the input information in this proposed scheme. Another SB control strategy was developed in [17], aiming at maximizing the performance of the SBs while solar and wind RSs are operating. Both generation and storage sources were guided by a dynamic tariff scheme. Aiming to optimize the performance of an SBs plant that serves a community of solar energy producers, the work in [24] proposed the control of domestic loads and RSs within this community. By applying this control, communities contributed to PG's ancillary services. The impact of the SBs and RSs of the consumer communities on the PG operation at periods of peak consumption and high intermittency was studied by [25]. Furthermore, [26] and [27] proposed the optimal control of SBs of energy communities aiming at

minimizing the total costs related to their degradation. Characteristics such as battery type, energy capacity, SB life cycle curve, and maximum output power were considered in [26], while in [27] the authors coordinated the operation of the SBs with the production of solar power, aiming to meet the PG needs. To ensure the energy balance between the energy consumption of communities and the generation of a wind farm, the authors in [28] performed the control of sodium-sulfur SBs connected to the PG. In addition to ensuring the energy balance, this control strategy aimed to mitigate disturbances in the supply network. A linear programming model was proposed by [29] to optimally size the SBs in a community of low voltage consumers aiming to save the energy bill. Moreover, the work has evaluated the different configurations for the allocation of SBs in the communities' distribution network.

The third direction includes works related to the management of appliances and the charging of EVs within energy communities. Thus, [30] proposed a pricing scheme called Real-Time Community Pricing (RTCP) to make the energy use of a community of customers more flexible in order to obtain a reduction in the total cost of electricity consumption. The work in [31] proposed a household load control scheme in a smart home community aiming to schedule the usage of appliances for the next day in periods of low tariff. Similarly, an energy management strategy for household loads and EVs was developed in [32] in order to reduce peak consumption and electricity bills. To improve the performance of electricity-gas-heat-cold sources in energy communities, [33] implemented a DR strategy that aims to reduce peak consumption in these communities, thereby ensuring the balance between generation and demand. Works related to implementing the DR strategies in communities, integrating the LF as an indicator of the efficient usage of electricity in the PG, can also be considered in this direction. For example, the authors in [16] proposed an optimization model for improving the LF of a community of smart homes by managing household loads that aim to mitigate the occurrence of new consumption peaks at off-peak hours. The authors in [34] aimed to improve the LF of a community of smart homes that adopted solar generation sources. Through these sources and the management of home appliances, savings in energy bills have been achieved for all homes. Also, a multi-objective model was developed in [35] that aimed to optimize the operation of both RSs and the fast charging of EVs in order to improve the LF. Finally, the research in [36] efficiently managed the power injection provided by RSs and EV fleets to the PG in order to increase the LF. In addition, this management strategy contributed to reducing the peak demand related to the consumption profile of the total number of consumers.

Table 1 summarizes the features studied and not studied by the works reviewed concerning our work. To this end, the following features are highlighted: (f1) financial and operational gains for DISCOs and consumers through energy management; (f2) reduction in peak demand considering the scheduling of both the usage of home appliances and the charging of EVs throughout the day; (f3) efficient performance of the SBs to manage the power supply by the PG;

(f4) improvement of the LF indicator related to the rational usage of electricity; (f5) reduction in the simultaneous usage of appliances with higher average power to avoid peak rebound or the occurrence of new peaks in demand at times with lower tariffs; and (f6) optimal coordination of SBs and DR strategy in communities of consumers with income diversity, and which contribute as a promising alternative to moderate the presence of RSs in the electrical grid of SCs.

Table 1. Overview of the reviewed works related to energy communities

Ref.	Author	Features					
		f1	f2	f3	f4	f5	f6
[10]	Dongol et al. (2018)	×	✓	✓	×	×	×
[11]	Zhou et al. (2020)	✓	✓	✓	×	×	×
[12]	Xing et al. (2019)	✓	✓	✓	×	×	×
[16]	Cerna & Contreras (2021)	×	✓	×	✓	✓	×
[17]	Singh et al. (2021)	✓	✓	✓	×	×	×
[19]	Fernandez et al. (2021)	✓	×	✓	×	×	×
[20]	Sasidharan et al (2017)	✓	×	✓	×	×	×
[21]	Elkadeem et al. (2020)	✓	✓	✓	×	×	×
[22]	Liang et al. (2020)	✓	×	✓	×	×	×
[23]	Duvignau et al. (2021)	✓	×	✓	×	×	×
[24]	Elkazaz et al. (2021)	✓	×	✓	×	×	×
[25]	Liu et al. (2017)	✓	✓	✓	×	×	×
[26]	Lee et al. (2020)	×	×	✓	×	×	×
[27]	Fortenbacher et al. (2017)	✓	×	✓	×	×	×
[28]	Moghaddan et al. (2018)	✓	×	✓	×	×	×
[29]	Weckesser et al. (2021)	✓	×	✓	×	×	×
[30]	Mamounakis et al. (2019)	✓	✓	×	×	×	×
[31]	Anees et al. (2021)	✓	✓	×	×	×	×
[32]	Cheng et al. (2020)	✓	✓	×	×	×	×
[33]	Li et al. (2021)	✓	✓	×	×	×	×
[34]	Cerna et al. (2021)	✓	✓	✓	✓	✓	×
[35]	Garcia-Villalobos et al. (2017)	✓	✓	×	✓	×	×
[36]	Trongwanichnam et al. (2019)	✓	✓	×	✓	×	×
	Proposed MILP Model	✓	✓	✓	✓	✓	✓

The works reviewed above show the strong presence of RSs in energy management strategies in consumer communities. On the one hand, in some studies, surplus power (solar or wind power) is traded as purchase/sale between consumer communities or between a given community and the PG with the support of DR strategies. In other works, this surplus power is

stored in the SBs and later traded according to a tariff scheme. Furthermore, in some other studies, the power of RSs provides ancillary services such as energy balance, voltage stability, etc. As can be seen, many works have contributed enormously to the development of these strategies and methodologies. However, proposals related to the efficient use of SBs and DR strategies in consumer communities (that disregard the use of RSs) to optimize the power coming from PG were not found. Therefore, since the use of RSs is consolidating within SCs, this existing gap should be filled. In this scenario, optimal alternatives such as NESCs will contribute to alleviating the disturbances caused by these sources. In an attempt to contribute to this area of research, we propose a MILP model to manage the electricity of an NESC by employing a price-based DR strategy in combination with a set of SBs. The proposed model aims to minimize: the total costs per energy consumption, the effect of peak rebound on the consumption profile, the energy waste through LF improvement, and the deep discharges of the SBs during their respective operational cycles. Operational constraints related to home appliances, EV batteries, SBs, and PG, are considered, while the consumption patterns of customers in each community are simulated using a Monte Carlo Algorithm (MCA). The performance of the proposed model is evaluated considering two NESCs, one of small scale and the other of large scale. In both cases, consumers are differentiated by household income and by the presence of individual SBs or SBs shared by consumers in a given community.

1.3. Contributions

The main contributions are itemized hereunder:

- Proposing a computationally-efficient MILP model that aims to determine the optimal operational scheme of the NESCs that are only provided by the PG.
- Finding an efficient schedule related to the usage of appliances and EVs charging in each residence considering the hourly preferences of consumers and without creating the peak rebound effect on the total consumption profile.
- Going against the conventional management schemes available in the literature that emphasize the presence of RSs, our proposal, based on NESCs, seeks to moderate the implementation of this type of schemes with RSs that, on a large scale, can compromise the reliability of the PG.
- Postponing investments in replacement or powering the PG infrastructure as a result of relieving its operational stress (i.e., reduction of maximum peak consumption and avoiding the occurrence of new peaks) during the day.

1.4. Paper organization

The remainder of the paper is as follows: the main assumptions, hourly preferences, simulation of consumption uncertainties, and operational scheme of NESCs are presented in Section 2; the proposed model and linearization process are detailed in Section 3; the results are

discussed in Section 4; and finally, the conclusions and limitations of this work, as well as future works, are shown in Section 5.

2. SIMULATION SETUP

In this section, the main assumptions and simulations associated with the operational performance of the NESCs are presented.

2.1. Assumptions

The main assumptions are:

- In NESCs, consumer communities are differentiated by household income. The income level in each household reflects the consumer's home appliance ownership [37]. For example, for the small-scale NESC scheme of Fig. 4, it is assumed that consumers in *Community 2* own a higher number of home appliances compared to *Community 1*.
- In consumer communities with a high presence of home appliances, the DR strategy will be applied. This strategy is guided through a tariff scheme with three levels (off-peak, intermediate and on-peak).
- The times of the day when consumers can use each appliance without compromising their comfort are represent by predefined values of hourly preferences $\beta''_{u,a,t}$. These values limit the scheduling of appliances to periods *t* that guarantee the comfort of communities with the highest number of domestic loads, e.g., *Community 2*.
- Each NESC is provided solely by PG. Thus, to support each consumer community, SBs are used. Therefore, the presence of RSs are disregarded as a source of supply for NESCs.
- It is assumed that all low-income consumer communities are supported by shared SBs. For example, in Fig. 4, all consumers in *Community 1* share a single SB. Furthermore, for high-income consumers, it is assumed that they are supported by individual SB. Still, in Fig. 4, in *Community 2*, each consumer is supported by an SB. It is worth mentioning that each individual SB (*Community 2*) has a smaller capacity compared to the capacity of the shared SB (*Community 1*).
- The NESC operation considers a day divided into 24 one-hour periods.
- Usage of household appliances disregards a logical sequence [16]. For example, the clothes dryer and washing machine can be scheduled for usage independently.
- All EVs present in NESCs only absorb power for battery charging.
- Household appliances (including EVs) are differentiated by working hours. Thus, there are home appliances with working hours less than one hour and greater than or equal to one hour, as reported in Tables 2, 3, and 4.

2.2. Hourly preferences for electricity consumption

As mentioned before, consumer communities are differentiated by household income. Thus, each consumer owns part of or all the appliances (including EVs) reported in Tables 2, 3, and 4 [34, 38 – 39]. Depending on daily needs and activities, each consumer can anticipate or postpone the periods of using appliances or charging the EV battery. These periods represent a certain level of flexibility in consumer comfort in exchange for financial gains on the energy bill. In this work, these periods are called hourly preferences and, are represented by the unit values of the binary parameter $\beta''_{u,a,t}$ (as shown in Fig. 1). Thus, when the customer considers wide flexibility of his/her hourly preferences (e.g., postponing usage of the electric shower for periods close to midnight or anticipating the usage of the washing machine for morning hours), their needs may be compromised, leading to discomfort. On the contrary, reduced flexibility in hourly preferences can concentrate energy consumption in a smaller number of periods on the day, which can lead to peaks in consumption (i.e., due to simultaneous usage of appliances related to cooking, cleaning, and entertainment activities). The values of $\beta''_{u,a,t}$ are predefined according to information collected and used in [16]. These $\beta''_{u,a,t}$ preference values will be used as key information in the MILP model for scheduling appliances and recharging EV batteries in order to obtain an optimal consumption profile, $\mathcal{O}^{c2}_{u,a,t}$.

Table 2. Appliances with working hours greater than or equal to 1 hour

	Home appliances a									
Features	Air Condit.	Freezer	Clothes Dryer	Computer	Light	TV	Electric Iron	Fan	DVD Player	Stereo
a	1	2	3	4	5	6	7	8	9	10
ϕ_a	1	1	1	1	1	1	1	1	1	1
β'_a	1	0	1	0	0	0	1	0	0	0
P_a	4.00	0.40	3.50	0.25	0.10	0.09	1.00	0.10	0.025	0.020
Ti_a^{av}	2	10	1	2	5	5	1	4	2	2
$\underline{Q}_a$	2	10	1	2	5	5	1	4	2	2
$\underline{Ti}_a$	0.25	0.50	0.50	0.50	0.25	0.50	0.25	0.50	0.25	0.25
Q_a	-	-	-	-	-	-	-	-	-	-

Table 3. Appliances with working hours less than 1 hour

	Home appliances a									
Features	Electric Faucet	Dishwasher	Coffee Maker	Resist. Oven	Electric Shower	Micro wave	Washing Machine	Vacuum Cleaner	Hair Dryer	Toaster
a	11	12	13	14	15	16	17	18	19	20
ϕ_a	0	0	0	0	0	0	0	0	0	0

β'_a	1	1	0	0	1	0	0	0	0	0
P_a	3.50	1.50	1.00	1.50	3.50	1.30	1.50	1.00	0.70	0.80
Ti_a^{av}	0.50	0.75	0.50	0.50	0.15	0.33	0.50	0.33	0.50	0.16
$\underline{Q}_a$	1	1	1	1	1	1	1	1	1	1
$\underline{Ti}_a$	-	-	-	-	-	-	-	-	-	-
Q_a	1	1	1	1	1	1	1	1	1	1

Table 4. EV technologies

Plug-in EVs			
A		21	
ϕ_a		-1	
β'_a		1	
BEV_u	20	24	32
P^e	4.0	4.0	4.0
$\underline{Ti}_u^e$	0.5	0.5	0.5
$\underline{Q}_u^c$	5.0	6.0	8.0

In Fig. 1, the hourly preferences $\beta''_{u,a,t}$ for each consumer in *Community 2* (see Fig. 4) are displayed. $\beta''_{u,a,t}$ = 1 indicates the periods *t* of the day when the appliance *a* (or EV) can be used by consumer *u* without harming his/her comfort. Otherwise, $\beta''_{u,a,t}$ = 0 represents the periods that compromise the consumer's comfort and therefore there is no usage of household appliances. Fig. 1 (a), (c), (e), and (g), on the left side, show the preferences $\beta''_{u,a,t}$ related to each consumer in *Community 2* in case he/she has an EV. For example, as reported in Table 5, only consumer 1 and 3 have one EV each. Thus, the hourly preferences $\beta''_{u,a,t}$ of these consumers are related to Figs. 1 (a) and (e), respectively. Therefore, during these periods ($\beta''_{u,a,t}$ = 1), consumer *u* can charge the EV battery without causing discomfort. On the right side, Figs. 1 (b), (d), (f), and (h) depict the $\beta''_{u,a,t}$ preferences related to the total number of household appliances, including the EV, present in each household in this community. It is worth mentioning that these hourly preferences can be customized for each consumer and be part of the information used by smart meters in the management of residential electricity consumption.

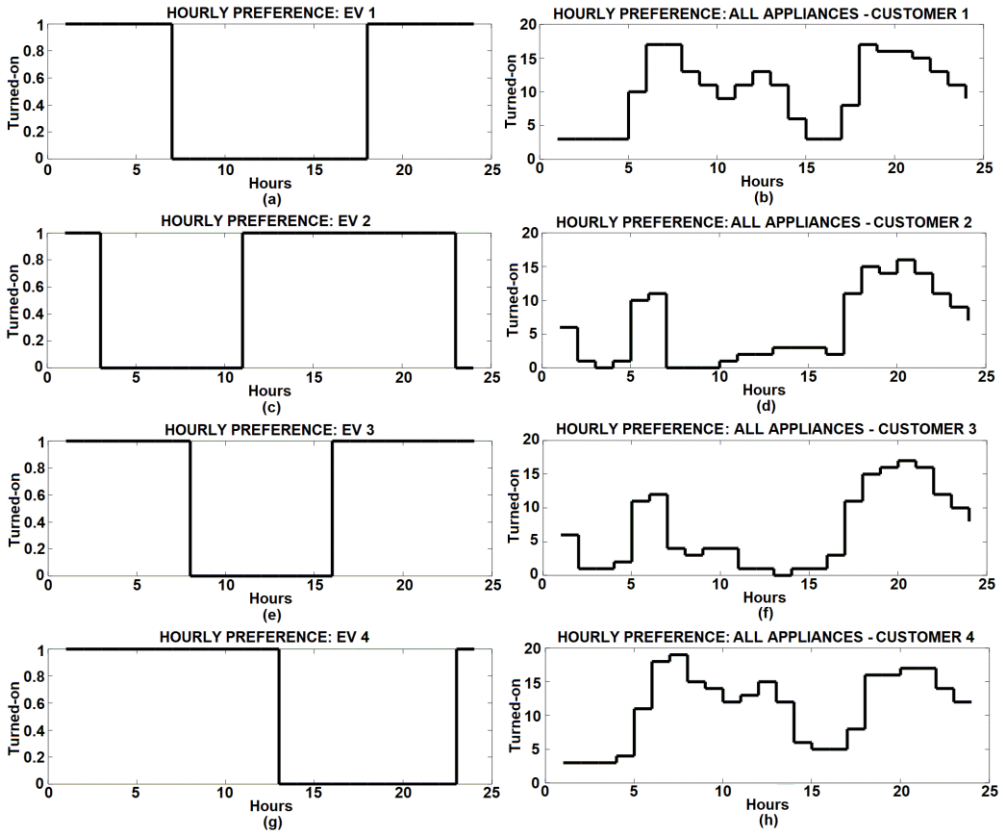

Figure 1. Hourly preferences of customers belonging to *Community 2*.

2.3. Simulation of uncertainties in consumption patterns

Since the electrical energy consumed changes hour-by-hour and consumer-by-consumer, determining the habitual consumption profile for each consumer during the day is a stochastic phenomenon. The simulation of the habitual consumption profiles of NESC consumers is carried out through the MCA [40−42]. The habitual consumption profile of each customer is formed by the sum of each consumption profile of household appliances (ϕ_a = 0 and ϕ_a = 1) and EVs (ϕ_a = –1) present in each household. The flowchart of the MCA is depicted in Figs. 2 and 3. Both Fig. 2 and 3 represent the first and second part of this flowchart, respectively. Note that the outputs (1), (2), (3), and (4) of the first part (Fig. 2) are the inputs of the second part (Fig. 3).

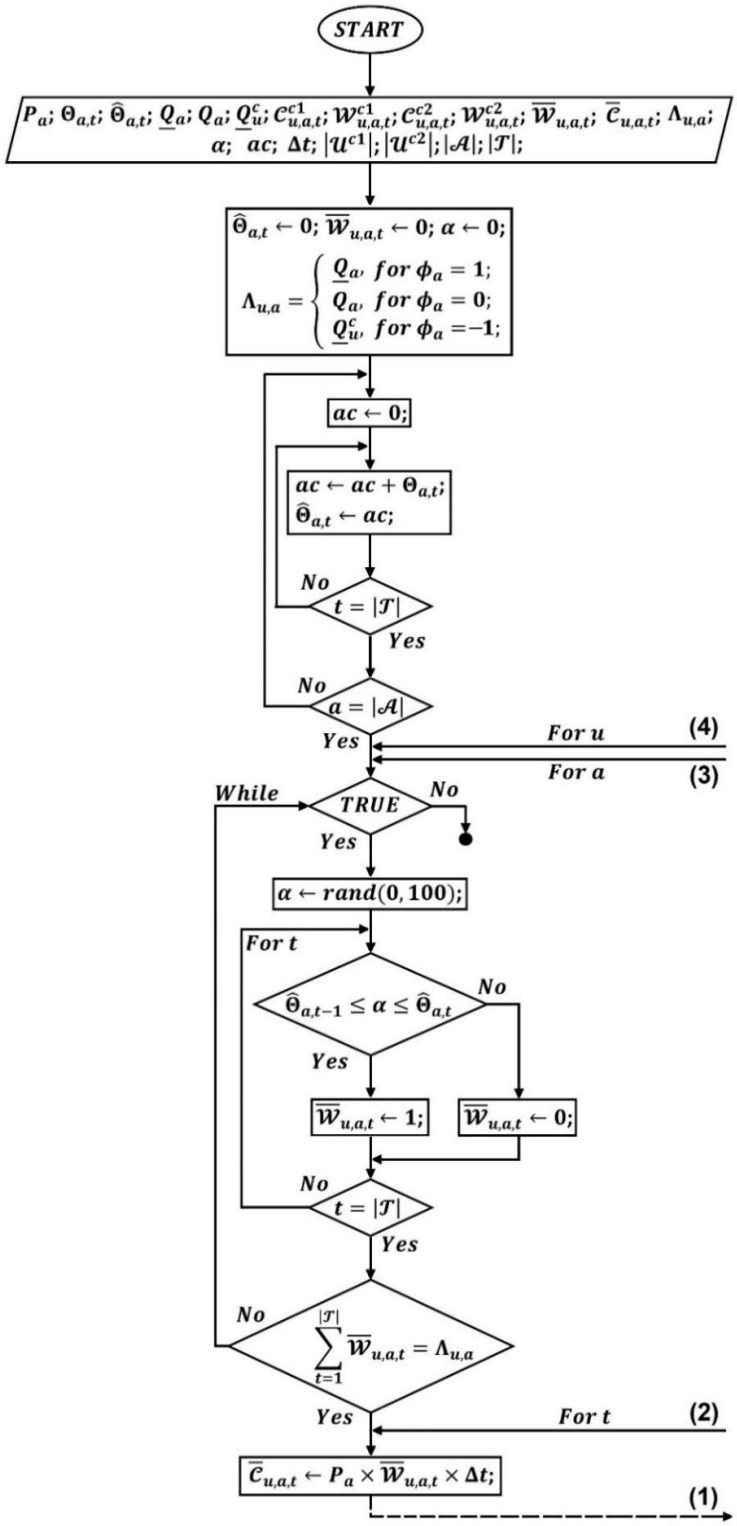

Figure 2. Part 1 of the MCA flowchart.

In Fig. 2 related to part 1, the MCA is run considering parameters such as the average power, P_a; the probability of turning-on appliance (or EV) a in each period t for electricity consumption, $\Theta_{a,t}$; the probability distribution related to the connection of household appliances (or EV) a in each period t for energy consumption, $\widehat{\Theta}_{a,t}$ [43, 44]; the minimum number of times that appliance a can be turned on for energy consumption in the day, $\underline{Q}_a$; mean value related to

the number of times that appliance *a* can be turned on for energy consumption in the day, Q_a; minimum number of times that the EV belonging to customer *u* can be turned on to recharge its battery in the day, $\underline{Q}_u^c$; habitual consumption profile associated with *Community 1*, $\mathcal{C}_{u,a,t}^{c1}$; on/off state of appliances and EVs belonging to *Community 1*, $\mathcal{W}_{u,a,t}^{c1}$; habitual consumption profile associated with *Community 2*, $\mathcal{C}_{u,a,t}^{c2}$; on/off state of appliances and EVs belonging to *Community 2*, $\mathcal{W}_{u,a,t}^{c2}$; on/off state of appliances and EVs present in both communities, $\overline{\mathcal{W}}_{u,a,t}$, (consisting of $\mathcal{W}_{u,a,t}^{c1}$ and $\mathcal{W}_{u,a,t}^{c2}$); habitual consumption profile, $\overline{\mathcal{C}}_{u,a,t}$ (composed of the corresponding profiles $\mathcal{C}_{u,a,t}^{c1}$ and $\mathcal{C}_{u,a,t}^{c2}$). Also, parameters like $\Lambda_{u,a}$; α random number; *ac* numerical accumulator; Δt time horizon; as well as the number of elements $|\mathcal{U}^{c1}|$, $|\mathcal{U}^{c2}|$, $|\mathcal{A}|$, and $|\mathcal{T}|$ associated with each set, $\mathcal{U}^{c1}$, $\mathcal{U}^{c2}$, $\mathcal{A}$, and $\mathcal{T}$, respectively, are considered. Next, parameters $\widehat{\Theta}_{a,t}$, $\overline{\mathcal{W}}_{u,a,t}$, α, and $\Lambda_{u,a}$ are initialized. Note that $\widehat{\Theta}_{a,t}$, $\overline{\mathcal{W}}_{u,a,t}$, and α are set to zero. Note also that $\Lambda_{u,a}$ can adopt the values of $\underline{Q}_a$, Q_a, and $\underline{Q}_u^c$ when ϕ_a turns out to be 1, 0, -1, respectively. After this MCA input information, an iterative process is performed for each appliance *a* and for each period *t*. For each iteration associated with appliance *a*, the *ac* accumulator is initialized to zero. Then, for each iteration *t*, $\Theta_{a,t}$ is added to the current value of *ac*, resulting in a new *ac*, which in turn will be assigned to $\widehat{\Theta}_{a,t}$. Iterations related to period *t* end once the condition $t = |\mathcal{T}|$ is verified for each iteration *a*. Similarly, the iterations associated with each appliance *a* end when condition $a = |\mathcal{A}|$ is met. Thereafter, three iterative processes related to each customer *u*, appliance *a*, and period *t* are performed. After the execution of each iteration *u*, related to the flow numbered with label (4), an iteration *a*, related to the flow numbered with the label (3), is done. Within this iteration *a*, an infinite loop is executed. In each iteration of this loop, a random number, α, between 0 and 100, is obtained. Next, an iterative process related to the set of periods $\mathcal{T}$ is performed, in which each α is evaluated under condition $\widehat{\Theta}_{a,t-1} \leq \alpha \leq \widehat{\Theta}_{a,t}$. If this condition is checked, then $\overline{\mathcal{W}}_{u,a,t}$ takes the value of 1; otherwise, $\overline{\mathcal{W}}_{u,a,t}$ is equal to 0. Then, condition $t = |\mathcal{T}|$ is evaluated. Iterations *t* end when the previous condition is met, otherwise the process continues to the next value of *t*. Once all the values for $\overline{\mathcal{W}}_{u,a,t}$ are obtained, the continuity condition of the infinity loop is evaluated. So, when $\sum_{t=1}^{|\mathcal{T}|} \overline{\mathcal{W}}_{u,a,t} = \Lambda_{u,a}$ is not checked, then, the loop continues to the next iteration. Otherwise, another iterative process related to the set of periods $\mathcal{T}$ is performed in order to determine the values of $\overline{\mathcal{C}}_{u,a,t}$ through the product of P_a, $\overline{\mathcal{W}}_{u,a,t}$, and Δt. This iterative process is associated with the flow numbered with label (2).

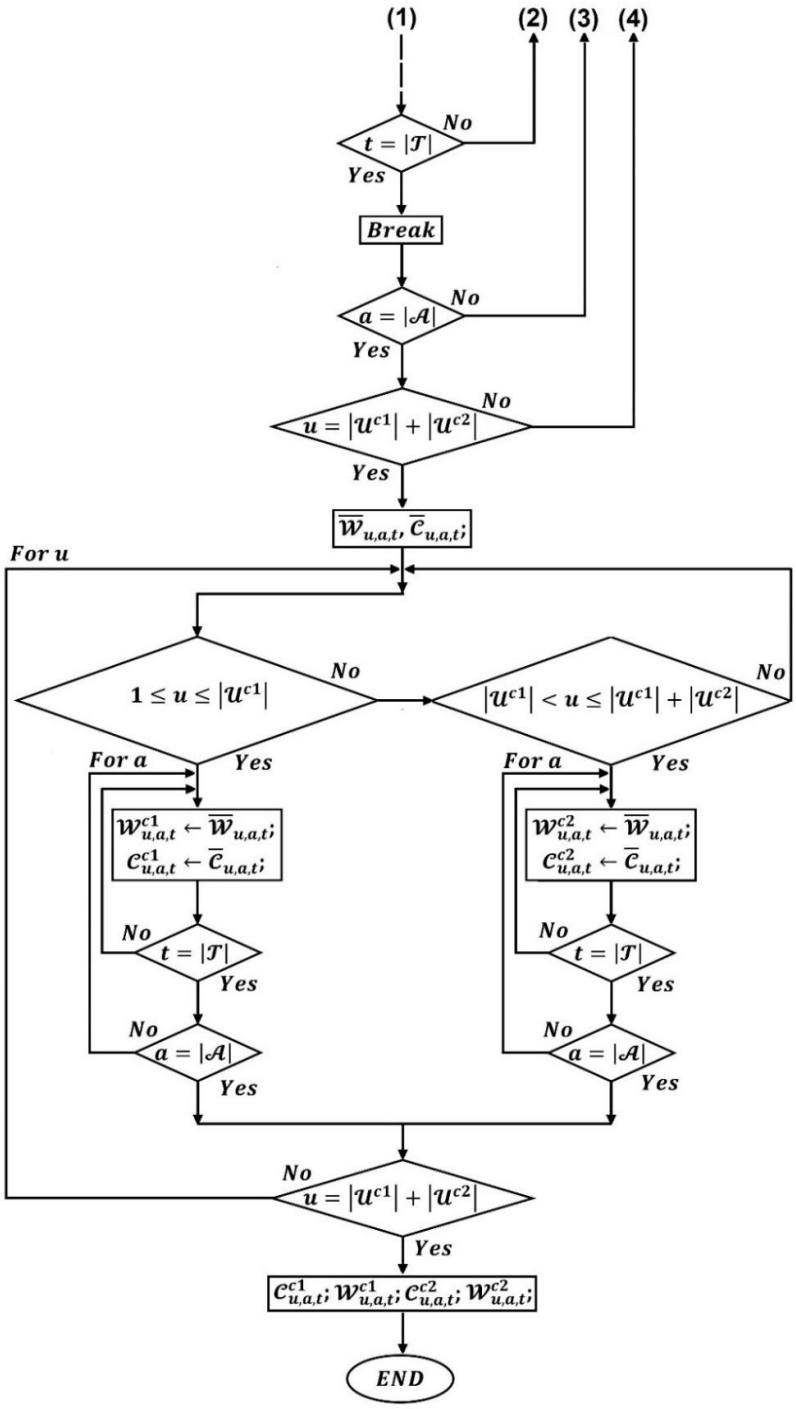

Figure 3. Part 2 of the MCA flowchart.

With the value of $\overline{c}_{u,a,t}$ calculated, the flow with label (1) directs the information to part 2 of the MCA flowchart as depicted in Fig. 3. Through this flow labeled (1), the iterative process for period t continues. In this sense, each value of t is evaluated under condition $t = |\mathcal{T}|$. When this condition is not met, then, the iterative process continues, otherwise, the infinite loop is broken. Next, condition, $a = |\mathcal{A}|$, is evaluated for each element of set $\mathcal{A}$. If this condition is not verified, then, the execution of the iterations continues, otherwise a new condition is evaluated. When this new condition, $u = |\mathcal{U}^{c1}| + |\mathcal{U}^{c2}|$, is not verified, the process continues, otherwise, the

values of $\overline{\mathcal{W}}_{u,a,t}$ and $\overline{\mathcal{C}}_{u,a,t}$ are obtained. After that, an iterative process related to the set of customers $\mathcal{U}$ is performed. This iterative process seeks to determine $\mathcal{W}^{c1}_{u,a,t}$ and $\mathcal{C}^{c1}_{u,a,t}$ (related to *Community 1*), and $\mathcal{W}^{c2}_{u,a,t}$ and $\mathcal{C}^{c2}_{u,a,t}$ (related to *Community 2*) from $\overline{\mathcal{W}}_{u,a,t}$ and $\overline{\mathcal{C}}_{u,a,t}$.

For each iteration *u*, initial condition $1 \leq u \leq |\mathcal{U}^{c1}|$ is evaluated. Note that this condition only considers residential customers in *Community 1*. When the previous condition is met, then, $\mathcal{W}^{c1}_{u,a,t}$ and $\mathcal{C}^{c1}_{u,a,t}$ are calculated within the iterative processes related to sets $\mathcal{T}$ and $\mathcal{A}$. Once the respective conditions $t = |\mathcal{T}|$ and $a = |\mathcal{A}|$ are met, the process continues to the next customer *u*. When the same condition $1 \leq u \leq |\mathcal{U}^{c1}|$ is not met, the new condition $|\mathcal{U}^{c1}| < u \leq |\mathcal{U}^{c1}| + |\mathcal{U}^{c2}|$ is evaluated. In this case, this new condition considers only the residential customers *u* of *Community 2*. If this last condition is not checked, then, another iteration for *u* is performed. Otherwise, the values of $\mathcal{W}^{c2}_{u,a,t}$ and $\mathcal{C}^{c2}_{u,a,t}$ are determined considering the iterative processes related to sets $\mathcal{T}$ and $\mathcal{A}$. Once the respective conditions, $t = |\mathcal{T}|$ and $a = |\mathcal{A}|$, are verified, the process continues and the current value of *u* is evaluated under condition $u = |\mathcal{U}^{c1}| + |\mathcal{U}^{c2}|$. While $u = |\mathcal{U}^{c1}| + |\mathcal{U}^{c2}|$ is not verified, the iterative process continues to the next value *u*. Otherwise, the process ends, and the values of $\mathcal{W}^{c1}_{u,a,t}$, $\mathcal{C}^{c1}_{u,a,t}$, $\mathcal{W}^{c2}_{u,a,t}$, and $\mathcal{C}^{c2}_{u,a,t}$ are obtained. Finally, the habitual consumption profiles, $\mathcal{C}^{c1}_{u,a,t}$ and $\mathcal{C}^{c2}_{u,a,t}$, are used in the operational constraints of the NESCs, described in the following section.

2.4. Operational scheme of the NESC

In this subsection, the power flow (supplied by PG, absorbed/injected by SBs and consumed by households) scheme related to the NESCs is described in detail. For practical purposes, the small-scale NESC will be used to describe this power flow, Fig. 4. As can be seen, this scheme considers two consumer communities both *Community 1* and *Community 2* with habitual consumption profile $\mathcal{C}^{c1}_{u,a,t}$ and $\mathcal{C}^{c2}_{u,a,t}$, respectively. All NESCs are only supplied by PG through P^{eg}_t power that is considered unidirectional. NESC does not consider the presence of RSs that send power back to the PG, therefore, reversing the flow of P^{eg}_t at certain times during the day will not be possible. The SBs are used by these consumer communities to support their electricity requirements, reducing the dependence on the power provided by PG, especially in periods of higher consumption. It is worth mentioning that the technical-operational restrictions allow the SBs to operate in coordination, keeping their state of charge close to total capacity and reducing deep discharges. In Fig. 4, *Community 1* uses an SB (with a capacity of $\mathcal{B}^{c1}$) that is shared by all consumers within this community. *Community 2* also uses SBs, but unlike *Community 1*, this community has one SB (with capacity $\mathcal{B}^{c2}_u$) for each consumer present. Components $P^{eg\_c1}_t$ and $P^{eg\_c2}_t$ of P^{eg}_t are considered bidirectional flows. Thus, depending on the consumption needs of each household and the state-of-charge (SOC) of the SBs ($\mathcal{E}^{c1}_t$ and $\mathcal{E}^{c2}_{u,t}$) during the day, these two-way flows between *Community 1* and *Community 2* can contribute to

mutual support. For example, for a given period *t* in which *Community 1* presents a high power demand, this would be met by $P_t^{eg\_c1}$ with P_t^{eg} and $P_t^{eg\_c2}$ components. In this case, the shared SB could inject $P_t^{inj\_c1}$ power to support the supply $P_{u,t}^{s\_c1}$ of the consumer units whenever $P_t^{eg\_c1}$ is insufficient. Otherwise, this SB could absorb $P_t^{abs\_c1}$ power to be stored. Still, in this case, the power $P_t^{eg\_c2}$ of *Community 2* will be the sum of the powers $P_{u,t}^{s\_c2}$ related to some or all of the individual SBs that inject power $P_{u,t}^{inj\_c2}$ depending on the consumption needs, $P_{u,t}^{h}$, of the households of this community.

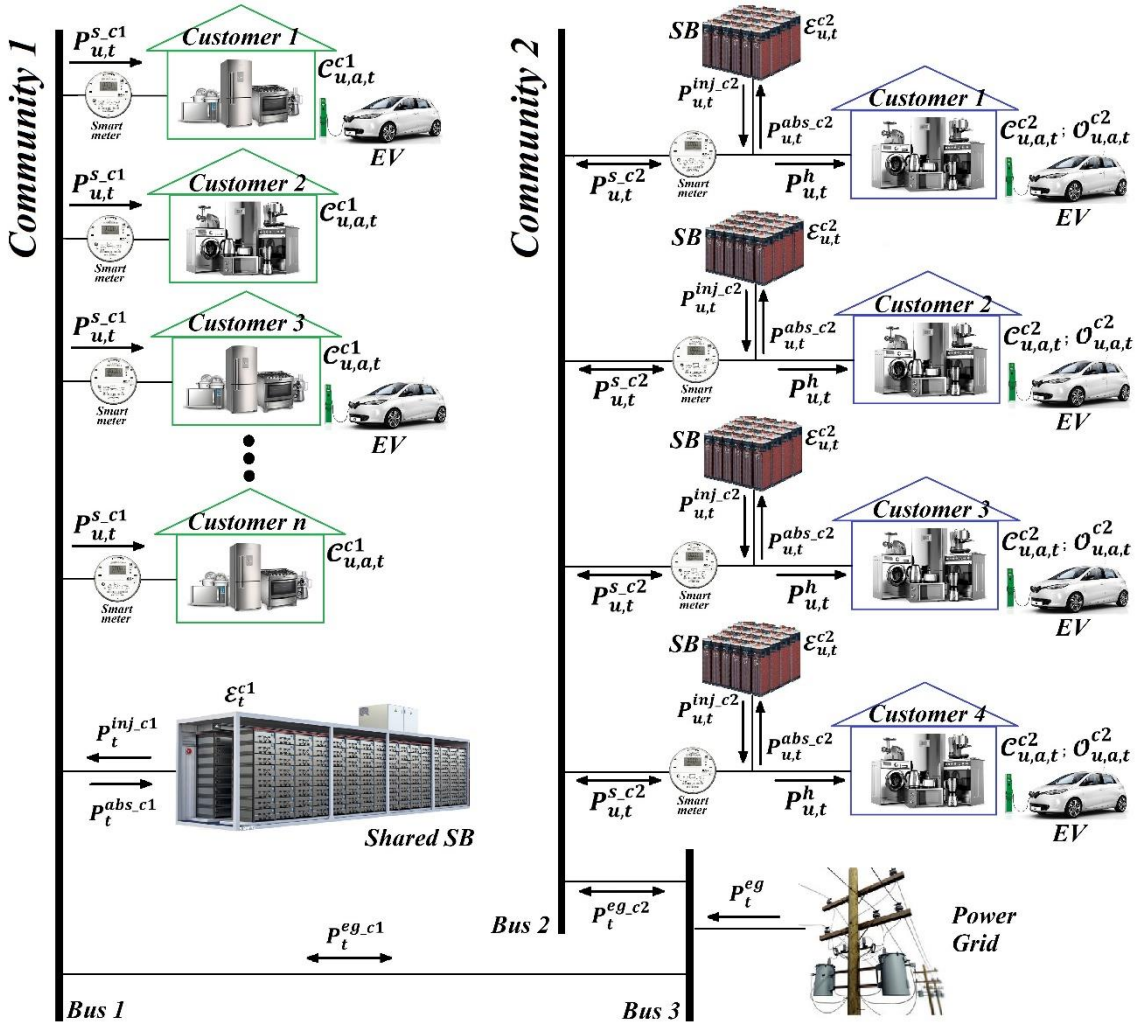

Figure 4. Power flow in the NESCs.

Still in Fig. 4, another case of mutual support is related to the consumption of *Community 2* when managed through a DR strategy (to get $\mathcal{O}_{u,a,t}^{c2}$ from $\mathcal{C}_{u,a,t}^{c2}$, since *Community 2* has a greater number of home appliances compared to *Community 1*). Here, reducing consumption peaks through efficient scheduling of home appliances usage and EVs charging contributes to relieving P_t^{eg} power. Meanwhile, part of the energy stored in the shared SB, $\mathcal{E}_t^{c1}$, (from *Community 1*) is supplied to *Community 2* through $P_t^{eg\_c1}$. In this case, $P_t^{eg\_c2}$ is equal to the sum of $P_t^{eg\_c1}$ and

P_t^{eg}. Thus, both SB and the household related to some or all consumer absorb power $P_t^{eg\_c2}$ through bidirectional power $P_{u,t}^{s\_c2}$. This bidirectionality of $P_{u,t}^{s\_c2}$ indicates that some fully charged SBs can support the supply of the remaining SBs and households in this community. These examples show the variation of power flows in the NESC as a function of the habitual consumption $\mathcal{C}_{u,a,t}^{c1}$ and the optimized consumption $\mathcal{O}_{u,a,t}^{c2}$ without the RSs presence that can congest the electricity supply network. Therefore, the daily operation of NESC turns out to be a highly complex problem and, in this sense, the improvement of its operation in order to meet the electricity requirements of consumers without compromising the lifetime of SBs and PG is a necessity.

3. PROPOSED MODEL

The mathematical formulation related to the problem of the optimal operation of NESCs is presented in this section.

3.1. Multi-objective function

$$min: \rho_1 \times \mathcal{F}_1 + \rho_2 \times \mathcal{F}_2 + \rho_3 \times \mathcal{F}_3 + \rho_4 \times \mathcal{F}_4 \quad (1)$$

In (1), functions $\mathcal{F}_1$, $\mathcal{F}_2$, $\mathcal{F}_3$, and $\mathcal{F}_4$ are the objectives to be minimized. The influence of each function on the solution of the problem is determined by weights ρ_1, ρ_2, ρ_3, and ρ_4, respectively. $\mathcal{F}_1$ is related to minimizing the energy bill of total consumers at NESC. Note that this function considers the P_t^{eg} power consumed by NESC in each period *t* together with the hourly rate λ_t. $\mathcal{F}_2$ aims to reduce, for each period *t*, the coincident usage of higher average power appliances. To efficiently reshape NESC's electricity consumption profile without peak rebound at low tariff times, i.e., LF improvement, $\mathcal{F}_3$ is calculated as the square of the difference between P_t^{eg} and $\tilde{P}^{eg}$. Finally, the lifecycle of the individual and shared SBs is optimized through $\mathcal{F}_4$. This optimization considers minimizing the difference between the SB's total capacity and its current SOC divided by this capacity. In the case of SB related to *Community 1* this term is given by ($\mathcal{B}^{c1}$ – $\mathcal{E}_t^{c1}$) / $\mathcal{B}^{c1}$ or 1 – ($\mathcal{E}_t^{c1}$ / $\mathcal{B}^{c1}$). Note that for a battery of capacity $\mathcal{B}^{c1}$, the reduction of $\mathcal{B}^{c1} - \mathcal{E}_t^{c1}$ implicitly allows maximizing $\mathcal{E}_t^{c1}$ for each period *t*. In this way, the number of complete SB discharges during the day can be reduced without harming its lifetime. Similarly, this reasoning has been applied to each SB *u* related to *Community 2*.

Each function mentioned above is presented below.

$$\mathcal{F}_1 = \sum_{\forall t \in \mathcal{T}} \lambda_t \times P_t^{eg}$$

$$\mathcal{F}_2 = \sum_{\forall u \in \mathcal{U}^{c2}} \sum_{\forall t \in \mathcal{T}} \theta'_{u,t}$$

$$\mathcal{F}_3 = \sum_{\forall t \in \mathcal{T}} \left(P_t^{eg} - \tilde{P}^{eg}\right)^2$$

$$\mathcal{F}_4 = \sum_{\forall t \in \mathcal{T}} \left(1 - \frac{\mathcal{E}_t^{c1}}{\mathcal{B}^{c1}}\right) + \sum_{\forall t \in \mathcal{T}} \sum_{\forall u \in \mathcal{U}^{c2}} \left(1 - \frac{\mathcal{E}_{u,t}^{c2}}{\mathcal{B}_u^{c2}}\right)$$

3.2. Operating constraints

The multi-objective function presented in (1) is subject to the set of technical constraints described below:

3.2.1. Power grid

The equality between the total power supplied by the PG, P_t^{eg}, and the sum of $P_t^{eg\_c1}$ and $P_t^{eg\_c2}$ is established through (2) for each period *t*.

$$P_t^{eg} = P_t^{eg\_c1} + P_t^{eg\_c2}; \forall t \in \mathcal{T} \quad (2)$$

3.2.2. Community 1

In (3), the power supplied to a given customer *u*, in each period *t*, $P_{u,t}^{s\_c1}$, is calculated as the sum of the energy consumption of all household appliances *a*, $\mathcal{C}_{u,a,t}^{c1}$, within that period *t*, divided by Δt. Through (4), the power balance between $P_t^{eg\_c1}$, $P_t^{inj\_c1}$ and $P_t^{abs\_c1}$, related to the shared SB, and $P_{u,t}^{s\_c1}$, associated with the total customers, is guaranteed.

$$P_{u,t}^{s\_c1} = \frac{1}{\Delta t} \times \sum_{\forall a \in \mathcal{A}} \mathcal{C}_{u,a,t}^{c1}; \forall u \in \mathcal{U}^{c1}, \forall t \in \mathcal{T} \quad (3)$$

$$P_t^{eg\_c1} + \left(P_t^{inj\_c1} - P_t^{abs\_c1}\right) = \sum_{\forall u \in \mathcal{U}^{c1}} P_{u,t}^{s\_c1}; \forall t \in \mathcal{T} \quad (4)$$

Binary variables $\alpha_t^{abs\_c1}$ and $\alpha_t^{inj\_c1}$ in (5) determine the injection or absorption state of the shared SB after its initial SOC, i.e., for $t > 1$. For variables $P_t^{inj\_c1}$ and $P_t^{abs\_c1}$, their maximum and minimum limits $\underline{P}^{inj\_c1}$ and $\overline{P}^{inj\_c1}$, and $\underline{P}^{abs\_c1}$ and $\overline{P}^{abs\_c1}$, are established by (6) and (7), respectively. In (8), the SOC of the SB, $\mathcal{E}_t^{c1}$, for $t = 1$, is set, considering the value of $\mathcal{E}^{o\_c1}$. The value of $\mathcal{E}_t^{c1}$ for $t > 1$ is calculated using (9). Furthermore, the charging and discharging cycles of the shared SB are limited through the lower and upper value $\underline{\gamma}^{c1} \times \mathcal{B}^{c1}$ and $\overline{\gamma}^{c1} \times \mathcal{B}^{c1}$ in (10), respectively [45]. In this equation, $\underline{\gamma}^{c1} \times \mathcal{B}^{c1}$ indicates the minimum energy level that the SOC, $\mathcal{E}_t^{c1}$, can reach and, $\overline{\gamma}^{c1} \times \mathcal{B}^{c1}$ the maximum energy level that this $\mathcal{E}_t^{c1}$ can reach so that the life of the SB is not compromised. Using (11), $\mathcal{E}_t^{c1}$ of the shared SB at the end of the day is obtained as a percentage $\overline{\gamma}^{c1}$ of its capacity, $\mathcal{B}^{c1}$.

$$\alpha_t^{abs\_c1} + \alpha_t^{inj\_c1} = 1; \forall t \in \mathcal{T}: t > 1 \quad (5)$$

$$\alpha_t^{inj\_c1} \times \underline{P}^{inj\_c1} \leq P_t^{inj\_c1} \leq \alpha_t^{inj\_c1} \times \overline{P}^{inj\_c1}; \forall t \in \mathcal{T} \quad (6)$$

$$\alpha_t^{abs\_c1} \times \underline{P}^{abs\_c1} \leq P_t^{abs\_c1} \leq \alpha_t^{abs\_c1} \times \overline{P}^{abs\_c1}; \forall t \in \mathcal{T} \quad (7)$$

$$\mathcal{E}_t^{c1} = \mathcal{E}^{o\_c1}; \forall t \in \mathcal{T}: t = 1 \quad (8)$$

$$\mathcal{E}_t^{c1} = \mathcal{E}_{t-1}^{c1} + \eta^{abs\_c1} \times P_t^{abs\_c1} \times \Delta t - \eta^{inj\_c1} \times P_t^{inj\_c1} \times \Delta t;\ \forall t \in \mathcal{T}: t > 1 \quad (9)$$

$$\underline{\gamma}^{c1} \times \mathcal{B}^{c1} \leq \mathcal{E}_t^{c1} \leq \overline{\gamma}^{c1} \times \mathcal{B}^{c1};\ \forall t \in \mathcal{T} \quad (10)$$

$$\mathcal{E}_t^{c1} = \overline{\gamma}^{c1} \times \mathcal{B}^{c1};\ \forall t \in \mathcal{T}: t = |\mathcal{T}| \quad (11)$$

3.2.3. Community 2

In (12), the power demand, $P_{u,t}^{h}$, by each consumer u in each period t is calculated considering the optimal profile, $\mathcal{O}_{u,a,t}^{c2}$. The energy balance between $P_{u,t}^{h}$ and the sum of $P_{u,t}^{s\_c2}$ and $(P_{u,t}^{inj\_c2} - P_{u,t}^{abs\_c2})$ is established in (13). (14) shows how the sum of $P_{u,t}^{s\_c2}$ for each customer u is equal to $P_t^{eg\_c2}$ for each period t.

$$P_{u,t}^{h} = \frac{1}{\Delta t} \times \sum_{\forall a \in \mathcal{A}} \mathcal{O}_{u,a,t}^{c2};\ \forall u \in \mathcal{U}^{c2}, \forall t \in \mathcal{T} \quad (12)$$

$$P_{u,t}^{s\_c2} + \left(P_{u,t}^{inj\_c2} - P_{u,t}^{abs\_c2}\right) = P_{u,t}^{h},; \forall u \in \mathcal{U}^{c2}, \forall t \in \mathcal{T} \quad (13)$$

$$P_t^{eg\_c2} = \sum_{\forall u \in \mathcal{U}^{c2}} P_{u,t}^{s\_c2};\forall t \in \mathcal{T} \quad (14)$$

The scheduling of appliances and EVs is performed using (15) and (16). (15) guarantees that household appliances a are not turned on in period t, in which hourly preferences are disregarded, $\beta''_{u,a,t} = 0$. Unlike (15), (16) establishes that household appliances a are turned on or not for period t with $\beta''_{u,a,t} = 1$.

$$\mathcal{W}_{u,a,t}^{ou} = 0; \forall u \in \mathcal{U}^{c2}, \forall a \in \mathcal{A}, \forall t \in \mathcal{T}: \beta''_{u,a,t} = 0 \quad (15)$$

$$\mathcal{W}_{u,a,t}^{ou} \leq 1; \forall u \in \mathcal{U}^{c2}, \forall a \in \mathcal{A}, \forall t \in \mathcal{T}: \beta''_{u,a,t} = 1 \quad (16)$$

(17) is related to household appliances a with higher average power, $\beta'_a = 1$. Thus, the number of times these appliances a are used in each period t, for each consumer u, is assigned to $\theta'_{u,t}$.

$$\theta'_{u,t} = \sum_{\forall a \in \mathcal{A}} \mathcal{W}_{u,a,t}^{ou} \times \beta''_{u,a,t} \times \beta'_a;\forall u \in \mathcal{U}^{c2}, \forall t \in \mathcal{T} \quad (17)$$

(18), and (19) are used to model the operating regime of appliances with working time less than 1 hour ($\phi_a = 0$). The number of times, Q_a, that appliance a, with $\phi_a = 0$, will be turned on for daily energy consumption is established in (18). (19) shows the calculation of the optimal consumption profile, $\mathcal{O}_{u,a,t}^{c2}$, for this type of appliance.

$$\sum_{\forall t \in \mathcal{T}} \mathcal{W}_{u,a,t}^{ou} \times \beta''_{u,a,t} = Q_a; \forall u \in \mathcal{U}^{c2}, \forall a \in \mathcal{A}: \phi_a = 0 \quad (18)$$

$$\mathcal{O}_{u,a,t}^{c2} = P_a \times \mathcal{W}_{u,a,t}^{ou} \times Ti_a^{av} \times \beta''_{u,a,t}; \forall u \in \mathcal{U}^{c2}, \forall a \in \mathcal{A}, \forall t \in \mathcal{T}: \phi_a = 0 \quad (19)$$

The operating regime of home appliances with working hours greater than or equal to 1 hour ($\phi_a = 1$) is simulated using (20) – (23). In (20), the minimum, $\underline{Q}_a$, and maximum, $\overline{Q}_a$, daily usage values of household appliances a are established. Likewise, in (21), the time interval,

$[\underline{Ti}_a, \overline{Ti}_a]$, of usage of each appliance *a* is also established. The optimal profile, $\mathcal{O}^{c2}_{u,a,t}$, of these appliances *a* is determined in (22). (23) guarantees the equality between Ti^{av}_a parameter and the total time, on the day, in which appliance *a* will be scheduled.

$$\underline{Q}_a \leq \sum_{\forall t \in \mathcal{T}} \mathcal{W}^{ou}_{u,a,t} \times \beta''_{u,a,t} \leq \overline{Q}_a; \forall u \in \mathcal{U}^{c2}, \forall a \in \mathcal{A}: \phi_a = 1 \quad (20)$$

$$\underline{Ti}_a \leq Ti^{on}_{u,a,t} \leq \overline{Ti}_a; \forall u \in \mathcal{U}^{c2}, \forall a \in \mathcal{A}, \forall t \in \mathcal{T}: \phi_a = 1 \quad (21)$$

$$\mathcal{O}^{c2}_{u,a,t} = P_a \times \mathcal{W}^{ou}_{u,a,t} \times Ti^{on}_{u,a,t} \times \beta''_{u,a,t}; \forall u \in \mathcal{U}^{c2}, \forall a \in \mathcal{A}, \forall t \in \mathcal{T}: \phi_a = 1 \quad (22)$$

$$\sum_{\forall t \in \mathcal{T}} \mathcal{W}^{ou}_{u,a,t} \times Ti^{on}_{u,a,t} \times \beta''_{u,a,t} = Ti^{av}_a; \forall u \in \mathcal{U}^{c2}, \forall a \in \mathcal{A}: \phi_a = 1 \quad (23)$$

(24) – (29) are related to each EV battery charging ($\phi_a = -1$). For each consumer *u*, in each period *t*, the SOC, $\mathcal{G}^{ev}_{u,t}$, of their EV battery is calculated, (24). Also, the charging time, $Ti^{e}_{u,t}$, in each period *t* is limited according to $\left[\underline{Ti}^{e}_{u}, \overline{Ti}^{e}_{u}\right]$, (25). Moreover, the number of times, in a day that an EV battery can be charged is determined by the $\underline{Q}^{c}_{u}$ and $\overline{Q}^{c}_{u}$ limits, (26). (27) assigns the values of $\mathcal{G}^{ev}_{u,t}$ to the optimal profile, $\mathcal{O}^{c2}_{u,a,t}$. The total SOC, $\mathcal{G}^{s}_{u}$, of the EV associated with the consumer *u* is calculated as the sum of SOC^{0}_{u} and $\mathcal{G}^{ev}_{u,t}$, (28). Finally, through (29), $\mathcal{G}^{s}_{u}$ is limited to not exceeding a percentage, ξ, of BEV_u capacity.

$$\mathcal{G}^{ev}_{u,t} = P^{e} \times \mathcal{W}^{ou}_{u,a,t} \times Ti^{e}_{u,t}; \forall u \in \mathcal{U}^{c2}, \forall a \in \mathcal{A}, \forall t \in \mathcal{T}: \phi_a = -1 \quad (24)$$

$$\underline{Ti}^{e}_{u} \leq Ti^{e}_{u,t} \leq \overline{Ti}^{e}_{u}; \forall u \in \mathcal{U}^{c2}, \forall t \in \mathcal{T} \quad (25)$$

$$\underline{Q}^{c}_{u} \leq \sum_{\forall t \in \mathcal{T}} \mathcal{W}^{ou}_{u,a,t} \leq \overline{Q}^{c}_{u}; \forall u \in \mathcal{U}^{c2}, \forall a \in \mathcal{A}: \phi_a = -1 \quad (26)$$

$$\mathcal{O}^{c2}_{u,a,t} = \mathcal{G}^{ev}_{u,t}; \forall u \in \mathcal{U}^{c2}, \forall a \in \mathcal{A}, \forall t \in \mathcal{T}: \phi_a = -1 \quad (27)$$

$$\mathcal{G}^{s}_{u} = SOC^{0}_{u} + \sum_{\forall t \in \mathcal{T}} \mathcal{G}^{ev}_{u,t}; \forall u \in \mathcal{U}^{c2} \quad (28)$$

$$\mathcal{G}^{s}_{u} \leq \xi \times BEV_u; \forall u \in \mathcal{U}^{c2} \quad (29)$$

(30) guarantees that the optimal consumption profile, $\mathcal{O}^{c2}_{u,a,t}$, does not present consumption peaks that exceed the consumption peak related to the habitual profile, $\mathcal{C}^{c2}_{u,a,t}$. The value $\mathcal{C}^{c2,max}$ represents the maximum value of $\mathcal{C}^{c2}_{t}$, which, in turn, was obtained by adding up the consumption, $\sum_{\forall u \in \mathcal{U}^{c2}} \sum_{\forall a \in \mathcal{A}} \mathcal{C}^{c2}_{u,a,t}$, related to each appliance *a* belonging to customer *u*.

$$\sum_{\forall u \in \mathcal{U}^{c2}} \sum_{\forall a \in \mathcal{A}} \mathcal{O}^{c2}_{u,a,t} \leq \mathcal{C}^{c2,max}; \forall t \in \mathcal{T} \quad (30)$$

SB performance related to consumer *u* is represented by (31) – (37). In (31), $\alpha^{abs\_c2}_{u,t}$ and $\alpha^{inj\_c2}_{u,t}$ are used to define, for each period *t*, the injection/absorption state of each SB *u*. The operating ranges $\left[\underline{P}^{inj\_c2}_{u}, \overline{P}^{inj\_c2}_{u}\right]$ and $\left[\underline{P}^{abs\_c2}_{u}, \overline{P}^{abs\_c2}_{u}\right]$ related to $P^{inj\_c2}_{u,t}$ and, $P^{abs\_c2}_{u,t}$ powers of each SB *u*, in a given period *t*, are established by (32) and (33). The initial SOC of SB *u* is

defined in (34). The SOC, $\mathcal{E}_{u,t}^{c2}$ (in period *t*) for each SB *u* is equal to the SOC, $\mathcal{E}_{u,t-1}^{c2}$ (in period *t* – 1) plus the energy resulting from injecting or absorbing state, in (35). In (36), the interval $[\underline{\gamma}_u^{c2} \times \mathcal{B}_u^{c2}, \overline{\gamma}_u^{c2} \times \mathcal{B}_u^{c2}]$ guarantees the discharging and charging limits of the SB during the day. Note that the percentage values $\underline{\gamma}_u^{c2}$ and $\overline{\gamma}_u^{c2}$ determine the SOC level of each SB *u* based on the $\mathcal{B}_u^{c2}$ capacity. Finally, (37) determines that the final SOC (i.e., for $t = |\mathcal{T}|$) of each SB *u* is equal to a percentage, $\overline{\gamma}_u^{c2}$, of its respective capacity, $\mathcal{B}_u^{c2}$.

$$\alpha_{u,t}^{abs\_c2} + \alpha_{u,t}^{inj\_c2} = 1; \forall u \in \mathcal{U}^{c2}, \forall t \in \mathcal{T}: t > 1 \tag{31}$$

$$\alpha_{u,t}^{inj\_c2} \times \underline{P}_u^{inj\_c2} \leq P_{u,t}^{inj\_c2} \leq \alpha_{u,t}^{inj\_c2} \times \overline{P}_u^{inj\_c2}; \forall u \in \mathcal{U}^{c2}, \forall t \in \mathcal{T} \tag{32}$$

$$\alpha_{u,t}^{abs\_c2} \times \underline{P}_u^{abs\_c2} \leq P_{u,t}^{abs\_c2} \leq \alpha_{u,t}^{abs\_c2} \times \overline{P}_u^{abs\_c2}; \forall u \in \mathcal{U}^{c2}, \forall t \in \mathcal{T} \tag{33}$$

$$\mathcal{E}_{u,t}^{c2} = \mathcal{E}_u^{o\_c2}; \forall u \in \mathcal{U}^{c2}, \forall t \in \mathcal{T}: t = 1 \tag{34}$$

$$\mathcal{E}_{u,t}^{c2} = \mathcal{E}_{u,t-1}^{c2} + \eta_u^{abs\_c2} \times P_{u,t}^{abs\_c2} \times \Delta t - \eta_u^{inj\_c2} \times P_{u,t}^{inj\_c2} \times \Delta t; \quad \forall u \in \mathcal{U}^{c2}, \forall t \in \mathcal{T}: t > 1 \tag{35}$$

$$\underline{\gamma}_u^{c2} \times \mathcal{B}_u^{c2} \leq \mathcal{E}_{u,t}^{c2} \leq \overline{\gamma}_u^{c2} \times \mathcal{B}_u^{c2}; \forall u \in \mathcal{U}^{c2}, \forall t \in \mathcal{T} \tag{36}$$

$$\mathcal{E}_{u,t}^{c2} = \overline{\gamma}_u^{c2} \times \mathcal{B}_u^{c2}; \forall u \in \mathcal{U}^{c2}, \forall t \in \mathcal{T}: t = |\mathcal{T}| \tag{37}$$

3.3. Linearization process

The proposed model presents a quadratic term in the function $\mathcal{F}_3$ and, products of variables in (22), (23), and (24). Therefore, the mathematical formulation detailed above corresponds to a mixed-integer nonlinear programming (MINLP) model and causes obstacles in finding the global solution of the problem.

By substituting $\mathcal{F}_3$, (22), (23), and (24) by their equivalent linear equations, the MINLP model becomes a mixed-integer linear programming (MILP) model. In this case, the polyhedral solution space guarantees the global solution of the problem. The linear (38) – (42) that replace $\mathcal{F}_3$ are based on [16, 39] that considers the technique of discretization of a quadratic function.

$$\mathcal{F}_3 = \sum_{\forall t \in \mathcal{T}} \left(P_t^{eg} - \tilde{P}^{eg}\right)^2 \cong \sum_{\forall t \in \mathcal{T}} \sum_{b=1}^{|\mathcal{B}|} \mathrm{X}_{t,b} \times \Delta \mathrm{Y}_{t,b}$$

$$\mathrm{Y}_t = P_t^{eg} - \tilde{P}^{eg}; \ \forall t \in \mathcal{T} \tag{38}$$

$$\mathrm{Y}_t^+ - \mathrm{Y}_t^- = \mathrm{Y}_t; \ \forall t \in \mathcal{T} \tag{39}$$

$$\mathrm{Y}_t^+ + \mathrm{Y}_t^- = \sum_{b=1}^{|\mathcal{B}|} \Delta \mathrm{Y}_{t,b}; \ \forall t \in \mathcal{T} \tag{40}$$

$$0 \leq \Delta \mathrm{Y}_{t,b} \leq \overline{\Delta}_t; \ \forall t \in \mathcal{T}, \forall b \in 1..|\mathcal{B}| \tag{41}$$

$$0 \leq \mathrm{Y}_t^+, \mathrm{Y}_t^-; \ \forall t \in \mathcal{T} \tag{42}$$

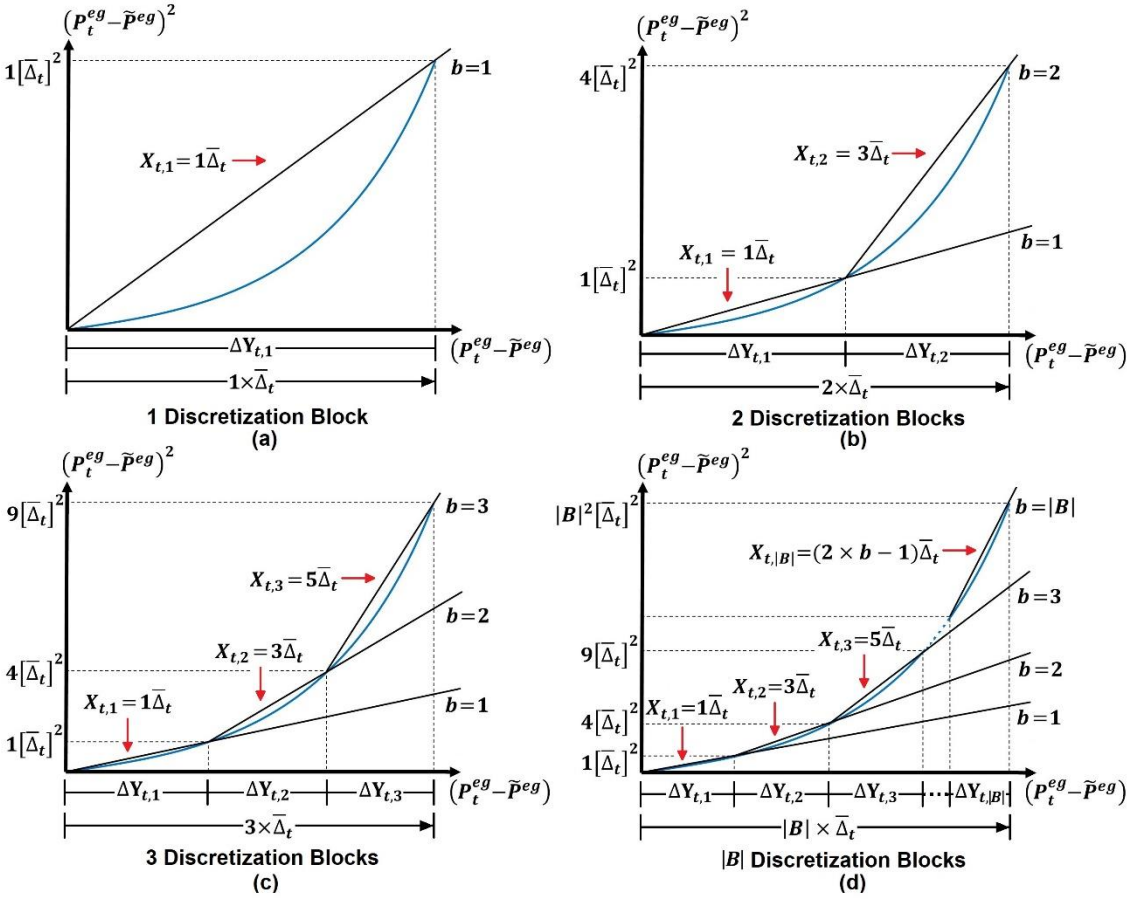

Figure 5. The discretization of $\mathcal{F}_3$.

Figs. 5 depicts the $\mathcal{F}_3$ quadratic function discretization technique. In the $\mathcal{F}_3$ function, notice that the quadratic term $\left(P_t^{eg} - \tilde{P}^{eg}\right)^2$ is replaced by the sum (from b = 1 to $|B|$) of the straight lines $\mathrm{X}_{t,b} \times \Delta\mathrm{Y}_{t,b}$ that pass through the coordinate origin and each one has a slope $\mathrm{X}_{t,b}$ equal to $(2 \times b - 1) \times \overline{\Delta}_t$. Still, in the sum, each value of b indicates the number of straight lines or discretization blocks (in black) used to obtain an approximation to the geometric form of the quadratic function (in blue). Based on this, Fig. 5 (a) depicts the first approximation to the function $\left(P_t^{eg} - \tilde{P}^{eg}\right)^2$ when a single discretization block is considered in the sum, i.e., b quals to 1. Through Figs. 5 (b) and (c), it can be seen that as the number of discretization blocks increases, the precision related to the geometric approximation between the set of blocks and the function $\left(P_t^{eg} - \tilde{P}^{eg}\right)^2$ also increases. Finally, Fig. 5 (d) shows a better approximation between the quadratic function and its discretized equivalent due to the increase from b to the value of $|B|$ discretization blocks. Therefore, depending on the values of P_t^{eg} and $\tilde{P}^{eg}$, an adequate number of discretization blocks can be predefined in order to obtain a more accurate result. It is worth mentioning that with the increase of b, the number of variables also increases, which may delay the execution time of the MILP model.

In the case of (22), (23), and (24), the linearization technique is based on the Big-M method [34, 46]. Thus, these equations are replaced by (43) – (46), and (47) – (49), respectively.

$$\mathcal{O}^{c2}_{u,a,t} = P_a \times \Delta Ti^{on}_{u,a,t} \times \beta''_{u,a,t}; \forall u \in \mathcal{U}^{c2}, \forall a \in \mathcal{A}, \forall t \in \mathcal{T}: \phi_a = 1 \quad (43)$$

$$\sum_{\forall t \in \mathcal{T}} \Delta Ti^{on}_{u,a,t} \times \beta''_{u,a,t} = Ti^{av}_{a}; \forall u \in \mathcal{U}^{c2}, \forall a \in \mathcal{A}: \phi_a = 1 \quad (44)$$

$$0 \leq -\Delta Ti^{on}_{u,a,t} + Ti^{on}_{u,a,t} \leq \mathcal{I} \times \left(1 - \mathcal{W}^{ou}_{u,a,t}\right); \forall u \in \mathcal{U}^{c2}, \forall a \in \mathcal{A}, \forall t \in \mathcal{T} \quad (45)$$

$$0 \leq \Delta Ti^{on}_{u,a,t} \leq \mathcal{I} \times \mathcal{W}^{ou}_{u,a,t}; \forall u \in \mathcal{U}^{c2}, \forall a \in \mathcal{A}, \forall t \in \mathcal{T} \quad (46)$$

$$\mathcal{G}^{ev}_{u,t} = P^e \times \Delta Ti^{e}_{u,t}; \forall u \in \mathcal{U}^{c2}, \forall a \in \mathcal{A}, \forall t \in \mathcal{T}: \phi_a = -1 \quad (47)$$

$$0 \leq -\Delta Ti^{e}_{u,t} + Ti^{e}_{u,t} \leq \mathcal{I} \times \left(1 - \mathcal{W}^{ou}_{u,a,t}\right); \forall u \in \mathcal{U}^{c2}, \forall a \in \mathcal{A}, \forall t \in \mathcal{T} \quad (48)$$

$$0 \leq \Delta Ti^{e}_{u,t} \leq \mathcal{I} \times \mathcal{W}^{ou}_{u,a,t}; \forall u \in \mathcal{U}^{c2}, \forall a \in \mathcal{A}, \forall t \in \mathcal{T} \quad (49)$$

Figs. 6 and 7 illustrate the application of this linearization technique to (43) – (46). For (47) – (49), the criterion is the same.

$$\Delta \boldsymbol{Ti}^{\boldsymbol{on}}_{\boldsymbol{u,a,t}} = \boldsymbol{Ti}^{\boldsymbol{on}}_{\boldsymbol{u,a,t}} \times \boldsymbol{\mathcal{W}}^{\boldsymbol{ou}}_{\boldsymbol{u,a,t}}$$

$$\begin{cases} \textit{If } \boldsymbol{\mathcal{W}}^{\boldsymbol{ou}}_{\boldsymbol{u,a,t}} = \boldsymbol{0}, \textit{then } \boxed{\Delta \boldsymbol{Ti}^{\boldsymbol{on}}_{\boldsymbol{u,a,t}} = \boldsymbol{0}} \\ \textit{If } \boldsymbol{\mathcal{W}}^{\boldsymbol{ou}}_{\boldsymbol{u,a,t}} = \boldsymbol{1}, \textit{then } \boxed{\Delta \boldsymbol{Ti}^{\boldsymbol{on}}_{\boldsymbol{u,a,t}} = \boldsymbol{Ti}^{\boldsymbol{on}}_{\boldsymbol{u,a,t}}} \end{cases}$$

$$\boldsymbol{0} \leq -\Delta \boldsymbol{Ti}^{\boldsymbol{on}}_{\boldsymbol{u,a,t}} + \boldsymbol{Ti}^{\boldsymbol{on}}_{\boldsymbol{u,a,t}} \leq \boldsymbol{\mathcal{I}} \times (\boldsymbol{1} - \boldsymbol{\mathcal{W}}^{\boldsymbol{ou}}_{\boldsymbol{u,a,t}})$$

$$\boldsymbol{0} \leq \Delta \boldsymbol{Ti}^{\boldsymbol{on}}_{\boldsymbol{u,a,t}} \leq \boldsymbol{\mathcal{I}} \times \boldsymbol{\mathcal{W}}^{\boldsymbol{ou}}_{\boldsymbol{u,a,t}}$$

$$\textit{If } \boldsymbol{\mathcal{W}}^{\boldsymbol{ou}}_{\boldsymbol{u,a,t}} = \boldsymbol{0}, \textit{then}$$

$$\begin{cases} \boldsymbol{0} \leq -\Delta \boldsymbol{Ti}^{\boldsymbol{on}}_{\boldsymbol{u,a,t}} + \boldsymbol{Ti}^{\boldsymbol{on}}_{\boldsymbol{u,a,t}} \leq \boldsymbol{\mathcal{I}} \\ \boldsymbol{0} \leq \Delta \boldsymbol{Ti}^{\boldsymbol{on}}_{\boldsymbol{u,a,t}} \leq \boldsymbol{0} \end{cases}$$

$$\Rightarrow \boxed{\Delta \boldsymbol{Ti}^{\boldsymbol{on}}_{\boldsymbol{u,a,t}} = \boldsymbol{0}}$$

$$\textit{If } \boldsymbol{\mathcal{W}}^{\boldsymbol{ou}}_{\boldsymbol{u,a,t}} = \boldsymbol{1}, \textit{then}$$

$$\begin{cases} \boldsymbol{0} \leq -\Delta \boldsymbol{Ti}^{\boldsymbol{on}}_{\boldsymbol{u,a,t}} + \boldsymbol{Ti}^{\boldsymbol{on}}_{\boldsymbol{u,a,t}} \leq \boldsymbol{0} \\ \boldsymbol{0} \leq \Delta \boldsymbol{Ti}^{\boldsymbol{on}}_{\boldsymbol{u,a,t}} \leq \boldsymbol{\mathcal{I}} \end{cases}$$

$$\Rightarrow \boxed{\Delta \boldsymbol{Ti}^{\boldsymbol{on}}_{\boldsymbol{u,a,t}} = \boldsymbol{Ti}^{\boldsymbol{on}}_{\boldsymbol{u,a,t}}}$$

Figure 6. Linearization of the product of two variables.

Fig. 6 shows that the product of $Ti^{on}_{u,a,t}$ and $\mathcal{W}^{ou}_{u,a,t}$, in (22) – (23) of the MINLP model, is being recast and only considers the value of $\Delta Ti^{on}_{u,a,t}$ in (43) – (44). Next, the value of $\Delta Ti^{on}_{u,a,t}$ is evaluated according to the values of the binary variable $\mathcal{W}^{ou}_{u,a,t}$. So, if $\mathcal{W}^{ou}_{u,a,t}$ = 0, then $\Delta Ti^{on}_{u,a,t}$ = 0. Otherwise, $\Delta Ti^{on}_{u,a,t} = Ti^{on}_{u,a,t}$. These same values must be verified by the $\Delta Ti^{on}_{u,a,t}$ variable when (45) – (46) are inserted in the proposed model. Still in Fig. 6, (45) – (46) are also being evaluated for $\mathcal{W}^{ou}_{u,a,t}$ values. If $\mathcal{W}^{ou}_{u,a,t}$ = 0, then the sum $-\Delta Ti^{on}_{u,a,t} + Ti^{on}_{u,a,t}$ is positive and less than the big value $\mathcal{I}$. At the same time, the $\Delta Ti^{on}_{u,a,t}$ interval shows that this variable takes the value of zero, i.e., $\Delta Ti^{on}_{u,a,t}$ = 0. Therefore, this evaluation corroborates the correspondence of $\Delta Ti^{on}_{u,a,t}$ = 0 since $\mathcal{W}^{ou}_{u,a,t}$ takes zero as its value. Furthermore, the geometric region described by (45) – (46) when

$\mathcal{W}_{u,a,t}^{ou}$ is zero is depicted in Fig. 7 (a). On the other hand, when $\mathcal{W}_{u,a,t}^{ou}$ = 1, then the sum $-\Delta Ti_{u,a,t}^{on} + Ti_{u,a,t}^{on}$ is equal to zero and $\Delta Ti_{u,a,t}^{on}$ varies between zero and the big value $\mathcal{I}$. Because $-\Delta Ti_{u,a,t}^{on} + Ti_{u,a,t}^{on}$ is equal to zero, then $\Delta Ti_{u,a,t}^{on} = Ti_{u,a,t}^{on}$, thus checking the correspondence of $\Delta Ti_{u,a,t}^{on} = Ti_{u,a,t}^{on}$ when $\mathcal{W}_{u,a,t}^{ou}$ = 1. Fig. 7 (b) shows the geometric region formed by (45) – (46) when $\mathcal{W}_{u,a,t}^{ou}$ = 1. For both Figs. 7 (a) and (b), the red line corresponds to the region that meets (45) – (46) when $\mathcal{W}_{u,a,t}^{ou}$ adopts 0 and 1, respectively.

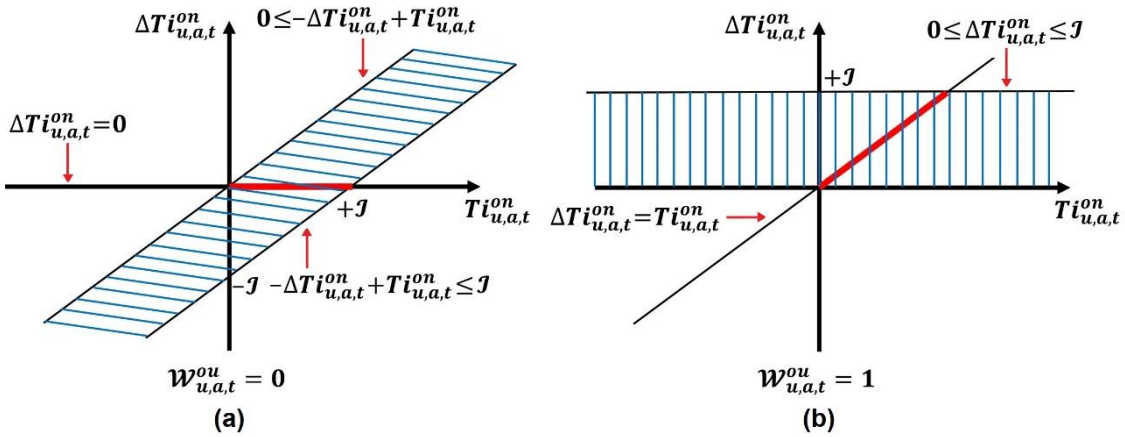

Figure 7. Geometry of linearized equations.

3.4. MILP model

Based on the linearization process detailed above, the proposed model adopts the following linearized formulation.

min (1)

subject to: (2) – (21), (25) – (37), (38) – (42), (43) – (46), (47) – (49).

4. RESULTS AND DISCUSSION

This section presents the results and discussion related to the evaluation of the operational scheme of the NESCs and their optimal management.

4.1. Basic data

The operational scheme in Fig. 4 is used to evaluate the performance of the MILP model. The appliances and EVs in Tables 2, 3 and 4 are the household loads considered in the NESCs. Moreover, the EVs are mainly differentiated by BEV_u capacities of 20 kWh, 24 kWh, and 32 kWh [47]. Table 5 shows, for both communities, the number of household appliances and EVs considered in each household. For example, in *Community 1*, only 4 customers have EVs (a = 21) with capacities of 20 kWh (customer 1), 32 kWh (customer 2) and 24 kWh (customers 4 and 5). All EV batteries start the day completely discharged. The habitual consumption profiles $\mathcal{C}_{u,a,t}^{c1}$ and $\mathcal{C}_{u,a,t}^{c2}$ are simulated using the MCA (depicted in Figs. 2 and 3) based on the above information. Because *Community 2* has the largest number of appliances per home, household

load scheduling will apply here, taking into account the hourly preferences, $\beta''_{u,a,t}$, [16] shown in Fig. 1. Moreover, the scheduling of appliances usage, and EV battery charging, are guided by an hourly tariff, λ_t, reported in Table 6 [48, 49].

Table 5. Types of home appliances and EV technology at each customer's home

Community 1	
Customer u	Home appliances and EVs a
1	1, 3, 4, 6, 7, 9, 10, 11, 12, 13, 15, 16, 17, 18, 19, 20, 21 (20 kWh)
2	10, 11, 12, 13, 14, 15, 16, 17, 18, 19, 20, 21 (32 kWh)
3	1, 2, 3, 4, 5, 6, 7, 8, 9, 10, 11, 12, 13
4	1, 2, 3, 4, 5, 6, 13, 14, 15, 16, 17, 18, 19, 20, 21 (24 kWh)
5	1, 2, 3, 4, 5, 6, 7, 8, 9, 10, 11, 12, 13, 14, 15, 16, 17, 18, 19, 20, 21 (24 kWh)
Community 2	
Customer u	Home appliances and EVs a
1	1, 2, 3, 4, 5, 6, 7, 8, 9, 10, 11, 12, 13, 14, 15, 16, 17, 18, 19, 20, 21 (20 kWh)
2	1, 2, 3, 4, 5, 6, 7, 8, 9, 10, 11, 12, 13, 14, 15, 16, 17, 18, 19, 20
3	1, 2, 3, 4, 5, 6, 7, 8, 9, 10, 11, 12, 13, 14, 15, 16, 17, 18, 19, 20, 21 (32 kWh)
4	1, 2, 3, 4, 5, 6, 7, 8, 9, 10, 11, 12, 13, 14, 15, 16, 17, 18, 19, 20

Table 6. Hourly energy tariffs

Periods	Level: Tariff
0h – 17h; 22h – 24h	Off peak: 0.22419 $/kWh
17h – 18h; 21h – 22h	Intermediate: 0.32629 $/kWh
18h – 21h	Peak: 0.51792 $/kWh

The technical data related to the SBs is reported in Table 7. Shared SB starts its operation (t = 0) fully charged about 10 kWh. All individual SBs have the same technical characteristics. Thus, these SBs with $\mathcal{B}_u^{c2}$ of 5 kWh start their operation fully discharged, $\mathcal{E}_u^{o\_c2}$ = 0. All SBs in NESCs are scheduled to achieve a final SOC equal to $\overline{\gamma}^{c1}$ (or $\overline{\gamma}_u^{c2}$) times the value of $\mathcal{B}^{c1}$ (or $\mathcal{B}_u^{c2}$) [34, 26]. In order to assess the efficient performance of SBs within NESC, especially at critical energy storage levels, the value of $\underline{\gamma}^{c1}$ is considered zero. In this way, the full performance of the SBs will be shown as part of the results. Also, these results will show the management scheme of household appliances and charging of EVs, as well as the remaining SBs, once a given SB is completely discharged. In the linearization process, constant $\mathcal{I}$, present in (45), (46), (48), and (49), and the total number of discretization blocks, $\mathcal{B}$, shown in (40) and (41), adopt the values of 100 and 15, respectively. Also, the maximum limit $\overline{\Delta}_t$ is calculated as $10/\mathcal{B}$ [46]. This MILP model employed a CPU time of about 50.2s and 120.4s for the small and large scale NESCs,

respectively, on a 2.67-GHz computer with 3GB of RAM and was implemented in AMPL [50] using CPLEX [51].

Table 7. Technical characteristics of the SBs

Community 1 – Shared SB	
Parameters	Values
$\underline{P}^{inj\_c1} / \overline{P}^{inj\_c1}$	2.5 kW / 3.2kW
$\underline{P}^{abs\_c1} / \overline{P}^{abs\_c1}$	2.2 kW / 3.2 kW
$\mathcal{B}^{c1} / \mathcal{E}^{o\_c1}$	10.0 kWh / 10.0kW
$\eta^{inj\_c1} / \eta^{abs\_c1}$	0.98 / 0.98
$\underline{\gamma}^{c1} / \overline{\gamma}^{c1}$	0.0 / 0.90
Community 2 – Individual SBs 1, 2, 3, and 4	
Parameters	Values
$\underline{P}_u^{inj\_c2} / \overline{P}_u^{inj\_c2}$	0.8 kW / 2.8 kW
$\underline{P}_u^{abs\_c2} / \overline{P}_u^{abs\_c2}$	0.8 kW / 2.8 kW
$\mathcal{B}_u^{c2} / \mathcal{E}_u^{o\_c2}$	5.0 kWh / 0.0 kWh
$\eta_u^{inj\_c2} / \eta_u^{abs\_c2}$	0.96 / 0.98
$\underline{\gamma}_u^{c2} / \overline{\gamma}_u^{c2}$	0.0 / 0.90

4.2. Analysis of weights

As shown in (1), functions $\mathcal{F}_1$, $\mathcal{F}_2$, $\mathcal{F}_3$, and $\mathcal{F}_4$ are multiplied by weights ρ_1, ρ_2, ρ_3, and ρ_4, respectively. In this analysis it is considered that each of the weights can adopt values between 0 and 1, specifically the set of values {0.25, 0.50, 0.75, 1.00}. Because $\mathcal{F}_4$ is related to the performance of all SBs in the NESCs, the focus of weight analysis will seek the smallest value of $\mathcal{F}_4$ function together with the values of the other functions when ρ_4 is fixed at 0.25, 0.50, 0.75, and 1.00 (in that order, as shown in Fig. 8), while the rest of the weights vary as a combination of the aforementioned set of values.

Fig. 8 (a) shows, in red, the values of $\mathcal{F}_4$, ranging from 70.88 to 74.61 when ρ_4 = 0.25. For ρ_4 = 0.50, the values of $\mathcal{F}_4$, in green, are greater than 74.00, reaching a maximum of 76.34, Fig. 8 (b). In Fig. 8 (c), the values of $\mathcal{F}_4$, in blue, range from 74.42 to 78.26, since ρ_4 is fixed at 0.75. Finally, when ρ_4 = 1.00, the values of $\mathcal{F}_4$, in black, show a minimum and maximum of 74.26 and 79.01, respectively, in Fig. 8 (d). Note that the minimum value of $\mathcal{F}_4$ (smallest number of deep discharges of the SBs) is depicted in Fig. 8 (a), where weights ρ_1, ρ_2, ρ_3, and ρ_4 adopt the values of 0.75, 0.50, 1.00, and 0.25, respectively. Therefore, these values are used in the analysis and discussion of NESCs at different scales.

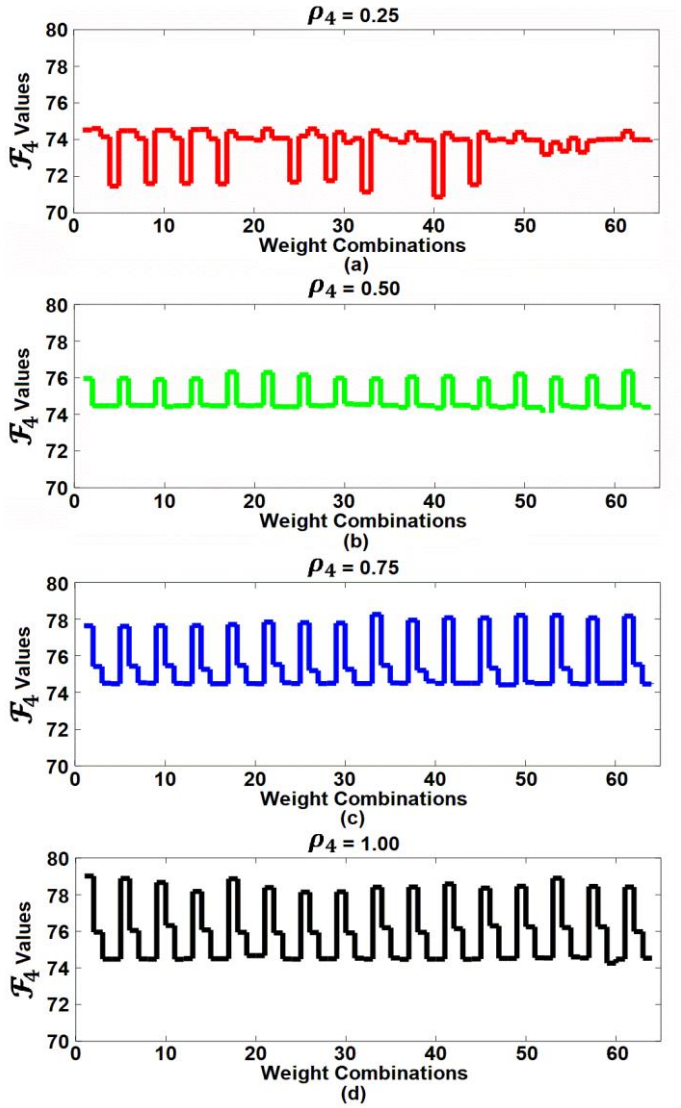

Figure 8. Values of $\mathcal{F}_4$ when ρ_4 is fixed to 0.25, 0.50, 0.75, and 1.00.

4.3. Small-scale NESC

For this NESC, the case studies to be analyzed are shown in Fig. 9. In *Case 1*, the proposed model is run considering the minimization of objectives related to functions $\mathcal{F}_1$, $\mathcal{F}_2$, and $\mathcal{F}_3$. *Case 2* considers the minimization of the aforementioned functions together with function $\mathcal{F}_4$. All functions are multiplied by their respective weights. Note that *Case 1* seeks the optimal performance of NESC with SB operation, but without taking into account the minimization of their deep discharges, i.e., without $\mathcal{F}_4$. In other words, this case only seeks to minimize the costs of customers in the communities, disregarding the lifetime of the SBs. On the contrary, *Case 2* is more complete due to the fact that it takes into account the improvement in the performance of SBs represented by $\mathcal{F}_4$ and its respective weight. For both cases, the information related to the weight values correspond to the values highlighted in the previous subsection, such as ρ_1 = 0.75, ρ_2 = 0.50, ρ_3 = 1.00, and ρ_4 = 0.25.

$$\textbf{Case 1} \begin{cases} \textbf{min:} \\ \rho_1 \times \mathcal{F}_1 + \rho_2 \times \mathcal{F}_2 + \rho_3 \times \mathcal{F}_3 \end{cases}$$

$$\textbf{Case 2} \begin{cases} \textbf{min:} \\ \rho_1 \times \mathcal{F}_1 + \rho_2 \times \mathcal{F}_2 + \rho_3 \times \mathcal{F}_3 + \rho_4 \times \mathcal{F}_4 \end{cases}$$

Figure 9. Case studies

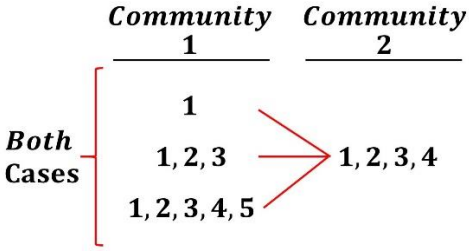

Figure 10. Assessment to be done for each case

Furthermore, for each case, the scheduling strategy of the appliances and EVs, as well as the operation of the SBs will be evaluated according to the gradual increase in the number of customers present in *Community 1*, with the number of customers in *Community 2* remaining constant, as depicted in Fig. 10. Note that, in both cases, the evaluation of the operational scheme of the NESC considers: a single customer (customer 1 in Table 5) in *Community 1* with all customers in *Community 2*; three customers (customer 1, 2, and 3 in Table 5) in *Community 1* with all customers in *Community 2*; and five customers (customer 1, 2, 3, 4, and 5 in Table 5) in *Community 1* with all customers in *Community 2*.

Fig. 11 shows in red, blue, and black, the power supplied by PG, P_t^{eg}, the power required/supplied by *Community 1*, $P_t^{eg\_c1}$, and the power required/supplied by *Community 2*, $P_t^{eg\_c2}$, respectively. In this figure, if $P_t^{eg\_c1}$ is positive, then, this power is requested by *Community 1*, otherwise, is provided by *Community 1*. The same criterion applies for $P_t^{eg\_c2}$. These powers, P_t^{eg}, $P_t^{eg\_c1}$, and $P_t^{eg\_c2}$, are shown in Figs. 11 (a) and (d); (b) and (e); and (c) and (f), when the number of consumers present in *Community 1* is 1, 3, and 5, respectively, for both cases. For 1 consumer, the power supplied by PG, P_t^{eg}, turns out to be constant and equal to 8.44 kW and 8.51 kW for *Cases 1* and *2*, respectively, without the occurrence of consumption peaks during the day. Moreover, in both cases, *Community 1* provides more power than *Community 2*, i.e., $P_t^{eg\_c1}$ is negative for a greater number of periods compared to $P_t^{eg\_c2}$. When the number of consumers increase to 3, the PG provides a constant power of 11.05 kW in *Case 1* and 11.11 kW in *Case 2*. Note that the power consumed, P_t^{eg}, by the NESCs is widely distributed throughout the day. Furthermore, the number of periods where *Community 2* provides power, that is, number of periods where $P_t^{eg_c2}$negative, increases is. Finally, for both cases, when the number of consumers is 5, P_t^{eg} remains almost constant at approximately 14 kW, with a peak demand of 24.65 kW in the period 19h – 20h. In this same period, *Community 2* provides its highest $P_t^{eg\_c2}$

power value of 11.20 kW. Note that for 5 consumers, the number of periods in which *Community 2* supplies power ($P_t^{eg\_c2}$ negative) is greater compared to *Community 1*.

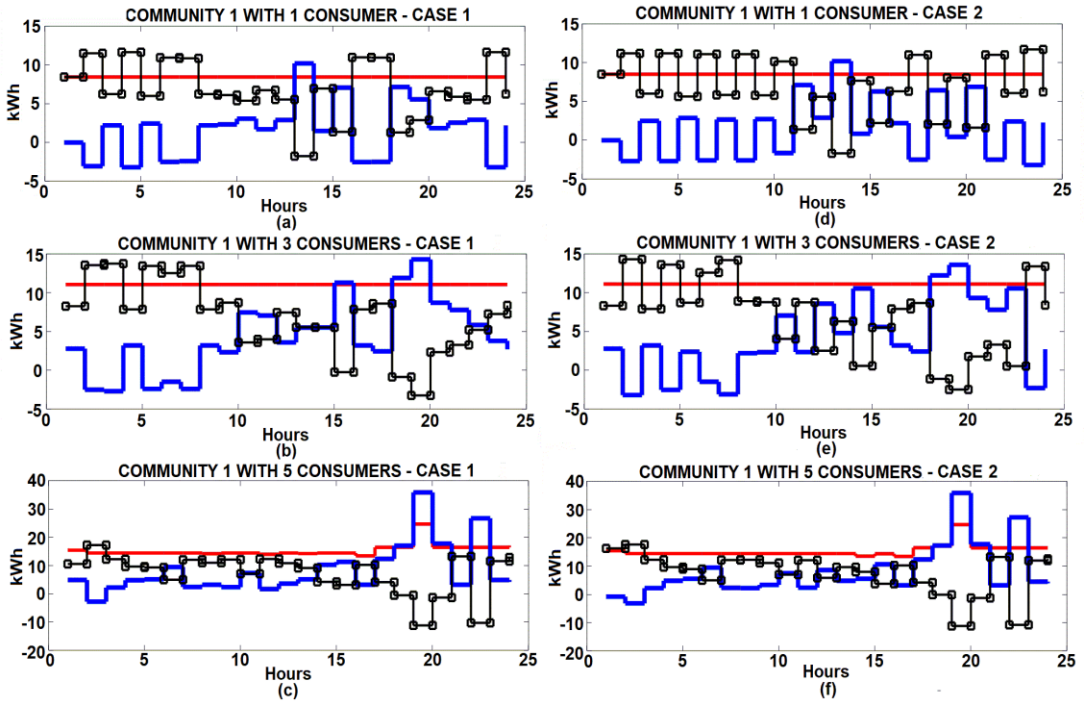

Figure 11. Values of P_t^{eg} (red), $P_t^{eg\_c1}$ (blue), and $P_t^{eg\_c2}$ (black), for both cases.

In Figs. 11 (c) and (f), for both cases, with the increase in the number of consumers, the peak value of $P_t^{eg\_c1}$ (blue) is mitigated by the scheduling of domestic loads and the use of energy stored in the SBs of *Community 2*. Consequently, the peak power related to P_t^{eg} (red) is reduced, contributing to minimize the stress of the supply network. In addition, in all cases, the LF value is always close to 1 due to the shift in the hours of usage of appliances and EVs recharge, in order to attenuate the consumption peak, avoiding its rebound in off-peak periods. For example, in *Case 1*, for 1 consumer in *Community 1*, both average and maximum demands are 8.44 kW, that is, LF is equal to 1. Similarly, for 3 consumers, both demands are 11.05 kW. For 5 consumers, the average demand is 15.42 kW and the maximum demand is 24.65 kW, i.e., the LF value is about 0.655. In this case, the LF value is affected by a high peak demand of 24.65 kW. Note that, even with the occurrence of this peak, the remaining periods present a homogeneous trend in electricity consumption in order to take advantage of idle periods of PG facilities and assets. These results show similar performances of NESCs in *Cases 1* and *2* because both cases aim to minimize functions $\mathcal{F}_1$, $\mathcal{F}_2$, and $\mathcal{F}_3$ (as depicted in Fig. 9) related to the optimal scheduling of appliances and EVs, strongly influenced by the shape of the profiles of P_t^{eg}, $P_t^{eg\_c1}$, and $P_t^{eg\_c2}$. Although *Case 2* seeks to minimize the deep discharge of the SBs through $\mathcal{F}_4$, this function weakly influences the shape of the power profiles already mentioned. The operational contribution of the $\mathcal{F}_4$ function (*Case 2*) is observed in Figs. 12 and 13 to be discussed below.

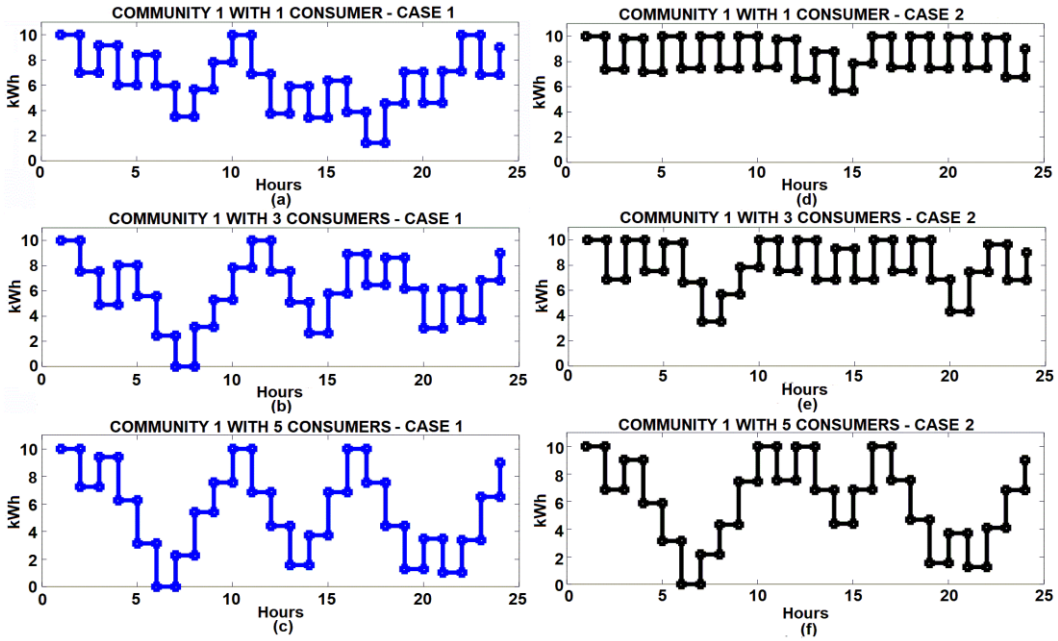

Figure 12. SOC of the shared SB, $\mathcal{E}_t^{c1}$, for *Case 1* (blue) and *Case 2* (black).

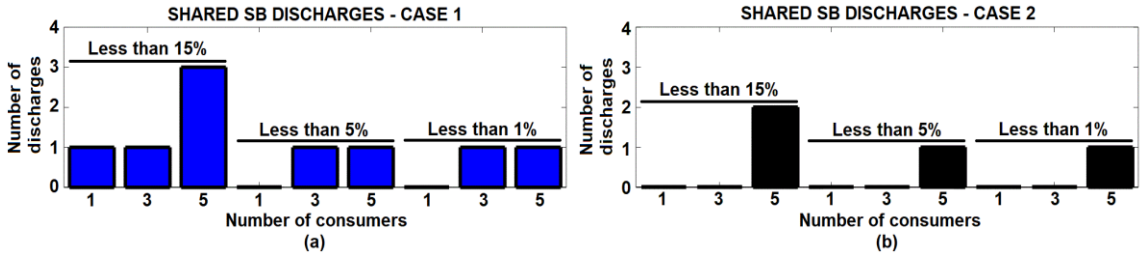

Figure 13. Number of Shared SB discharges for *Case 1* (blue) and *Case 2* (black).

Fig. 12 depicts the values of SOC, $\mathcal{E}_t^{c1}$, of the shared SB, for both cases. The SOC in blue is related to *Case 1*, while the SOC in black is related to *Case 2*. In all cases, the starting SOC is equal to $\mathcal{B}^{c1}$, and the ending SOC is scheduled to be 90% of $\mathcal{B}^{c1}$. Figs. 12 (a) and (d) show the SOC of the shared SB when 1 consumer is present in *Community 1*. In *Case 1*, the highest discharge of the SB is done in the period 17h – 18h, reaching an SOC of 1.43 kWh. In *Case 2*, the highest discharge of the same SB reaches an SOC of 5.58 kWh. In this latter case, note how the proposed model seeks to keep the SB's SOC close to its $\mathcal{B}^{c1}$ capacity. When 3 consumers are present in *Community 1*, the SOC of the shared SB is depicted in Figs. 12 (b) and (e). In *Case 1*, the greatest discharge occurs in the period 6h – 7h; in this period the SB is completely discharged. On the contrary, in *Case 2*, the higher SB discharges allows reaching an SOC close to 4 kWh, in periods 7h – 8h and 20h – 21h, and, in the rest of the periods, the SOC is kept close to $\mathcal{B}^{c1}$. Finally, for a heavy load of 5 consumers, both Figs. 12 (c) and (f) show a similar SOC. A slight difference appears in the period 10h – 15h. Within this period, the greatest discharge of the SB, in *Case 1*, reaches an SOC less than 2 kWh. For *Case 2*, the greatest discharge results in an SOC greater than 4 kWh. These results for both cases show the different performance of the shared SB when $\mathcal{F}_4$ is considered (or not) in the objective function. Thus, although in *Case 2* (Fig. 12 (f)), the

function $\mathcal{F}_4$ is being considered in the objective function, the smallest value of its respective weight ρ_4, given the high energy demand of *Community 1* with 5 consumers, does not represent a differentiated result due to this high domestic load, leading to a similar performance to *Case 1* (Fig. 12 (c)). The influence of the number of consumers present in *Community 1* is evident in Figs. 12 (a) and (d), and Figs. 12 (b) and (e). For example, for a single consumer present in *Community 1*, i.e., low domestic load, *Case 1* (Fig. 12 (a)), which disregards $\mathcal{F}_4$, presents energy discharges below half the capacity of SB. In *Case 2* (Fig. 12 (d)), which consider $\mathcal{F}_4$, the energy discharges are above half of the SB capacity. Furthermore, in *Cases 1* and *2* of Figs. 12 (b) and (e), it is possible to observe that for the increase in the number of consumers in *Community 1*, *Case 2* (Fig. 12 (e)) shows the appearance of deeper discharges compared to Fig. 12 (d). Therefore, this fact corroborates the influence of the number of consumers on the energy request from shared SB, even considering $\mathcal{F}_4$ (less weight compared to the other functions).

In Fig. 13, for both *Cases 1* (blue bars) and *2* (black bars), statistical data related to the number of discharges less than 15%, 5%, and 1% of the SB capacity are presented. For *Case 1*, when *Community 1* has 1 consumer, 3 consumers, and 5 consumers, the number of times the shared SB SOC is less than 15% of its capacity corresponds to 1, 1, and 3, respectively. These last values, in *Case 2*, are smaller. Thus, the number of times corresponds to 0, 0, and 2, respectively. Next, for both *Cases 1* and *2*, the number of times the SOC is less than 5% is also depicted in Fig. 13. For 1 consumer, there are no discharges lower than 5%; for 3 consumers, *Case 1* shows a discharge, and *Case 2* does not show discharges; and when there are 5 consumers present in *Community 1*, the number of discharges for both cases is equal to 1. Finally, for both *Cases 1* and *2*, when the SB SOC is close to complete discharge (i.e., less than 1%), it is observed that with 1 consumer present in *Community 1* there are no discharges; with 3 consumers, *Case 1* presents a complete discharge and in *Case 2* there are no SB discharges; and with 5 consumers, for both cases, the SB presents a single complete discharge. This fact corroborates how *Case 2* contributes to guaranteeing the optimization of the lifetime of the SB by reducing its number of discharges while the number of consumers in *Community 1* increases, demanding greater support for the SB.

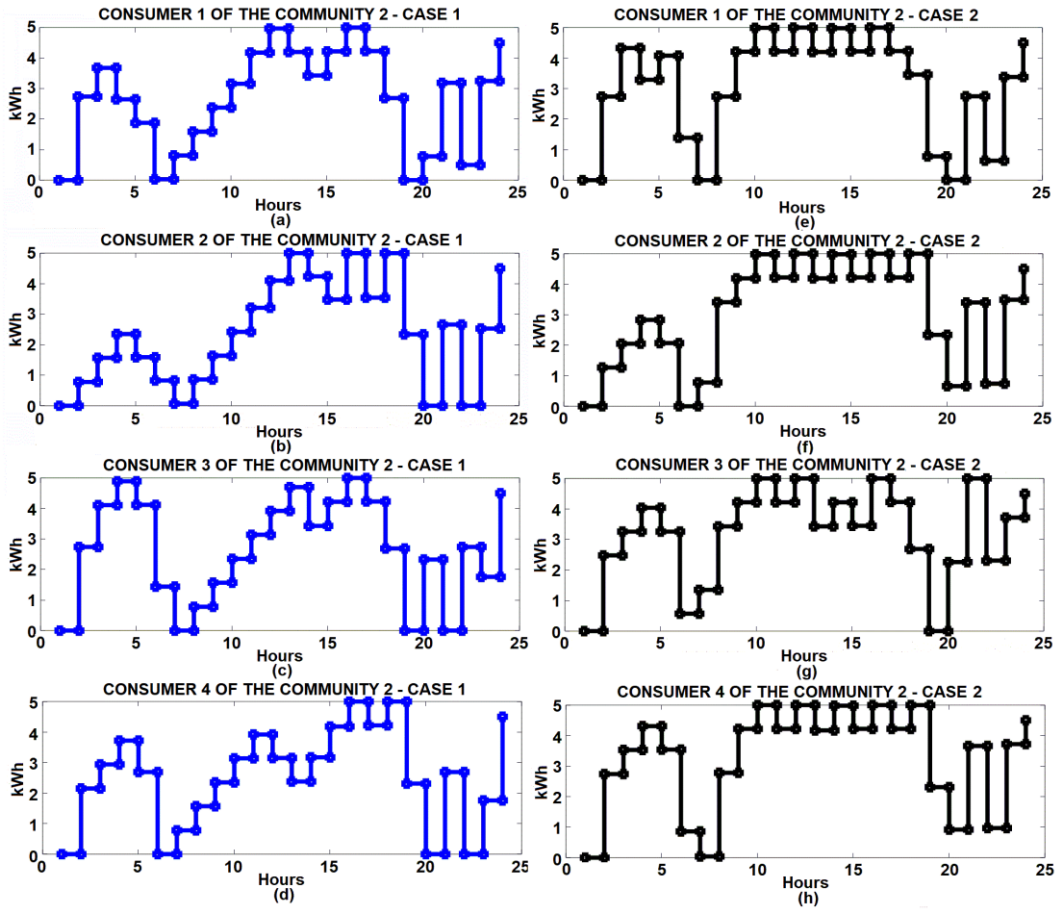

Figure 14. SOC of SBs related to consumers present in *Community 2* in both cases.

Similarly, Fig. 14 shows the SOC values, in blue and black, of the SB related to each consumer in *Community 2*, for both cases. All SBs start fully discharged and end with SOCs equal to 90% of $\mathcal{B}_u^{c2}$. Note that the consumers' SBs, in *Case 1*, Figs. 14 (a) – (d), present a minimum number of total discharges equal to 2, during the day. In *Case 2*, Figs. 14 (e) – (h), the minimum number of total discharges is equal to 1. Also, in this case, there are periods when the SOC is below 20% of $\mathcal{B}_u^{c2}$, Fig. 14 (e), in period 22h – 23h; Fig. 14 (f), in periods 20h – 21h and 22h – 23h; Fig. 14 (g), in period 6h – 7h; and Fig. 14 (h), in periods 20h – 21h and 22h – 23h. In these peak and intermediate periods, the SOC of the SBs does not reach full discharge. As can be seen in Fig. 14, *Case 2* seeks to reduce, during the day, the number of complete discharges in the SB of each consumer present in *Community 2*. Although, for both cases, each SB starts its operation completely discharged, in the following periods the greatest contribution to bring the SOC value near to the maximum capacity of the SB over a long period of time is given by *Case 2*.

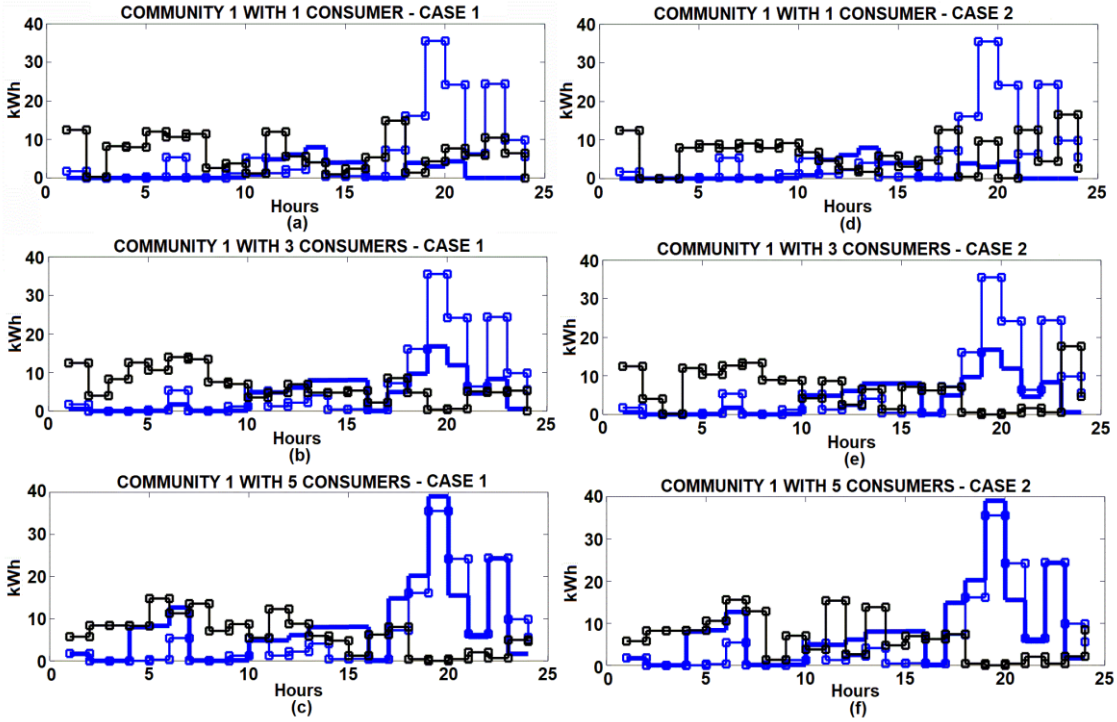

Figure 15. Habitual profile $\mathcal{C}_{u,a,t}^{c1}$ (in blue without squares) related to *Community 1*. Habitual profile $\mathcal{C}_{u,a,t}^{c2}$ (in blue with squares) and optimal profile $\mathcal{O}_{u,a,t}^{c2}$ (in black with squares) both related to *Community 2*.

Fig. 15 depicts the habitual consumption profiles, $\mathcal{C}_{u,a,t}^{c1}$ (in blue) and $\mathcal{C}_{u,a,t}^{c2}$ (in blue with squares) related to *Community 1* and *2*, respectively, as well as the optimal profile, $\mathcal{O}_{u,a,t}^{c2}$, (in black with squares) obtained by scheduling domestic loads and EVs in *Community 2*. For all cases, $\mathcal{C}_{u,a,t}^{c1}$ increases according to the number of consumers present in *Community 1*, $\mathcal{C}_{u,a,t}^{c2}$ remains the same, and $\mathcal{O}_{u,a,t}^{c2}$ reschedules consumption of *Community 2* according to the number of consumers in *Community 1*, SOCs of all SBs in the NESCs, and hourly rate, in order to mitigate the increase in peak demand and obtain a wide distribution of demand, P_t^{eg}, provided by the PG to the NESCs. According to the increase in the number of consumers present in *Community 1*, electricity consumption within the peak hours related to the $\mathcal{O}_{u,a,t}^{c2}$ profile (of *Community 2*) is reduced, and the household loads as well as the battery charging of the EVs are shifted to off-peak hours, considering the hourly preferences, $\beta_{u,a,t}''$, without creating new consumption peaks in P_t^{eg}. In Fig. 15, as the objective is to reshape the consumption profile of the total number of consumers to reduce the energy bill, avoid the coincident usage of appliances and minimize electricity waste, the $\mathcal{F}_4$ function does not influence consumption profiles due to being associated with the lifetime of the SBs. Therefore, for both *Cases 1* and *2*, the optimal consumption profile associated with *Community 2* will portray similar results, i.e., the strategy for scheduling the times for using appliances and charging EVs will be for periods with lower electricity rates. Note that in Figs. 15 (a) – (f), the scheduling strategy seeks to reduce the energy consumption of *Community*

2 within the peak period in order to alleviate the peak consumption of the total consumers (of both communities) when the peak consumption of *Community 1* progressively increases.

In Table 8, the financial costs related to the total electricity consumption are reported for each number of consumers present in *Community 1* (e.g., one consumer, 3 consumers, and 5 consumers). It is worth mentioning that when *Community 1* considers 3 consumers, the notation (1, 2, 3) corresponds to consumer 1, consumer 2, and consumer 3 whose home appliances and EVs are shown in Table 5. In this way, when *Community 1* has a single consumer (lower domestic load), the total cost related to the habitual consumption corresponds to 11.40$ ($\mathcal{C}_{u,a,t}^{c1}$ profile of *Community 1*) + 57.718$ ($\mathcal{C}_{u,a,t}^{c2}$ profile of *Community 2*) which turn out to be 69.118$. Still here, the total cost for electricity consumption considering *Case 1* corresponds to 11.40$ ($\mathcal{C}_{u,a,t}^{c1}$ profile of *Community 1*) + 40.63$ ($\mathcal{O}_{u,a,t}^{c2}$ profile of *Community 2*) which is equal to 52.03$. Also, considering *Case 2*, the total cost corresponds to 11.40$ ($\mathcal{C}_{u,a,t}^{c1}$ profile *Community 1*) + 41.244$ ($\mathcal{O}_{u,a,t}^{c2}$ profile of *Community 2*) which results in 52.644$. Another example is related to the case of greater domestic load, that is, when *Community 1* has 5 consumers. Here, the total cost for the habitual consumption results from the sum of 65.672$ ($\mathcal{C}_{u,a,t}^{c1}$ profile of *Community 1*) + 57.718$ ($\mathcal{C}_{u,a,t}^{c2}$ profile of *Community 2*) which is 123.39$. For *Case 1*, the total cost for electricity consumption corresponds to the sum of 65.672$ ($\mathcal{C}_{u,a,t}^{c1}$ profile of *Community 1*) + 34.982$ ($\mathcal{O}_{u,a,t}^{c2}$ profile of *Community 2*) which results in 100.65$. Finally, for *Case 2*, the total cost for electricity consumption corresponds to the sum of 65.672$ ($\mathcal{C}_{u,a,t}^{c1}$ profile of *Community 1*) + 34.645$ ($\mathcal{O}_{u,a,t}^{c2}$ profile of *Community 2*) which results in 100.32$.

Note that, in Table 8, in *Community 2*, the total cost for *Cases 1* and *2* are approximate values. However, any of these values (obtained from the $\mathcal{O}_{u,a,t}^{c2}$ profile) is lower compared to the financial savings associated with the $\mathcal{C}_{u,a,t}^{c2}$ profile. It is worth mentioning that these cases are distinguished by the operational performance of the SBs during the day that, at the same time, depending on the number of consumers present in the communities. Therefore, the optimality of the proposed model is based on the cost savings of the total number of consumers, the operability of the SBs and how both aspects influence the P_t^{eg} profile during the day, i.e., no energy wastage due to the mitigation of demand peaks. Also, note that in the higher domestic load scenario (increase in consumers in *Community 1* and decrease in peak consumption in *Community 2*), SBs have a sever requirement, especially during the peak period, consequently leading to a greater demand for P_t^{eg} and the appearance of peaks in this period.

Table 8. Electricity consumption costs

Community 1		*Community 2*			
Number of consumers	$\mathcal{C}_{u,a,t}^{c1}$ ($)	Number of consumers	$\mathcal{C}_{u,a,t}^{c2}$ ($)	*Case 1* $\mathcal{O}_{u,a,t}^{c2}$ ($)	*Case 2* $\mathcal{O}_{u,a,t}^{c2}$ ($)

1 (1)	11.40	4 (1, 2, 3, 4)	57.718	40.63	41.244
3 (1, 2, 3)	34.026	4 (1, 2, 3, 4)	57.718	36.922	34.858
5 (1, 2, 3, 4, 5)	65.672	4 (1, 2, 3, 4)	57.718	34.982	34.645

4.4. Large-scale NESC

In order to corroborate the large-scale applicability of the MILP model, a set of 14 communities supported with shared and individual SBs, considering *Case 2* (with ρ_1 = 0.75, ρ_2 = 0.50, ρ_3 = 1.00, and ρ_4 = 0.25), has been implemented. Table 9 reports the number of home appliances *a* and the ownership (or not) of EV (*a* = 21) per consumer belonging to each community. For instance, *Communities 1* and *5*, supported with shared SBs, have 3 and 4 consumers, respectively. In both communities, only 2 consumers have EV with a capacity of 20 kWh and 32 kWh. Furthermore, in each community, most consumers own a different number of home appliances *a*. Table 10 presents the SB capacity associated with each of the 14 communities. Note that each *Community 1*, *2*, *3*, *4*, *5*, *6*, *7*, and *8* is supported by an SB shared by their respective consumers. In the rest of the 14 communities, such as *9*, *10*, *11*, *12*, *13*, and *14*, each consumer is supported by an SB. In addition, all shared SBs start their daily operation fully charged, $\mathcal{E}^{o\_c1}$ = 10 kWh; $\mathcal{E}^{o\_c2}$ = 15 kWh; $\mathcal{E}^{o\_c3}$ = 10 kWh; $\mathcal{E}^{o\_c4}$ = 12 kWh; $\mathcal{E}^{o\_c5}$ = 10 kWh; $\mathcal{E}^{o\_c6}$ = 10 kWh; $\mathcal{E}^{o\_c7}$ = 15 kWh; and $\mathcal{E}^{o\_c8}$ = 12 kWh. On the contrary, the individual SBs start their operation fully discharged, $\mathcal{E}_1^{o\_c9} = \mathcal{E}_2^{o\_c9} = \mathcal{E}_3^{o\_c9}$ = 0 kWh; $\mathcal{E}_1^{o\_c10} = \mathcal{E}_2^{o\_c10} = \mathcal{E}_3^{o\_c10}$ = 0 kWh; $\mathcal{E}_1^{o\_c11} = \mathcal{E}_2^{o\_c11} = \mathcal{E}_3^{o\_c11} = \mathcal{E}_4^{o\_c11}$ = 0 kWh; $\mathcal{E}_1^{o\_c12} = \mathcal{E}_2^{o\_c12} = \mathcal{E}_3^{o\_c12} = \mathcal{E}_4^{o\_c12}$ = 0 kWh; $\mathcal{E}_1^{o\_c13} = \mathcal{E}_2^{o\_c13} = \mathcal{E}_3^{o\_c13}$ = 0 kWh; and $\mathcal{E}_1^{o\_c14} = \mathcal{E}_2^{o\_c14} = \mathcal{E}_3^{o\_c14}$ = 0 kWh. Technical characteristics such as injection/absorption power and the charging/discharging efficiency of the individual and shared SB are the same as those reported in Table 7.

Table 9. Types of home appliances and EV technology in each home community

Communities with shared SB		
Community	Number of consumers *u*	Home appliances and EVs *a*
1	3	Consumer 1: 1, 3, 4, 6, 7, 9, 10, 11, 12, 13, 15, 16, 17, 18, 19, 20, 21 (20 kWh); Consumer 2: 10, 11, 12, 13, 14, 15, 16, 17, 18, 19, 20, 21 (32 kWh); Consumer 3: 1, 2, 3, 4, 5, 6, 7, 8, 9, 10, 11, 12, 13.
2	4	Consumer 1: 1, 3, 4, 6, 7, 9, 10, 11, 12, 13, 15, 16, 17, 18, 19, 20, 21 (20 kWh) Consumer 2: 1, 2, 3, 4, 5, 6, 7, 8, 9, 10, 11, 12, 13; Consumer 3: 10, 11, 12, 13, 14, 15, 16, 17, 18, 19, 20, 21 (32 kWh); Consumer 4: 1, 2, 3, 4, 5, 6, 7, 8, 9, 10, 11, 12, 13.
3	3	Consumer 1: 1, 3, 4, 6, 7, 9, 10, 11, 12, 13, 15, 16, 17, 20, 21 (20 kWh);

		Consumer 2: 1, 3, 4, 6, 7, 9, 10, 11, 12, 13, 15, 16, 17, 18, 19, 20, 21 (20 kWh); Consumer 3: 1, 4, 6, 10, 11, 12, 13, 15, 16, 17, 18, 19, 20, 21 (20 kWh).
4	3	Consumer 1: 1, 3, 4, 6, 7, 9, 10, 11, 12, 13, 15, 16, 17, 18, 19, 20, 21 (20 kWh); Consumer 2: 1, 3, 4, 6, 7, 9, 10, 13, 15, 16, 17, 18, 20, 21 (20 kWh); Consumer 3: 1, 3, 4, 10, 13, 15, 16, 17, 18, 19, 20, 21 (32 kWh)
5	4	Consumer 1: 1, 3, 4, 6, 7, 9, 10, 11, 12, 13, 15, 16, 17, 18, 19, 20, 21 (20 kWh); Consumer 2: 1, 2, 3, 4, 5, 6, 7, 8, 9, 10, 11, 12, 13, 14, 15, 17, 19, 20; Consumer 3: 10, 11, 12, 13, 14, 15, 16, 17, 18, 19, 20 , 21 (32 kWh); Consumer 4: 1, 2, 3, 4, 5, 6, 7, 8, 9, 10, 11, 12, 13, 14, 15, 17, 18, 19, 20
6	3	Consumer 1: 1, 3, 4, 11, 12, 13, 15, 16, 17, 18, 19, 20, 21 (20 kWh); Consumer 2: 10, 11, 12, 13, 14, 15, 16, 17, 18, 19, 20 , 21, (32 kWh); Consumer 3: 1, 2, 3, 4, 5, 6, 7, 8, 9, 10, 11, 12, 13, 14, 15, 17, 18, 19, 20.
7	3	Consumer 1: 1, 3, 4,, 6, 7, 9, 10 11, 12, 13, 15, 16, 17, 18, 19, 20, 21 (20 kWh); Consumer 2: 10, 11, 12, 13, 14, 15, 16, 17, 18, 19, 20 , 21, (32 kWh); Consumer 3: 1, 2, 3, 6, 7, 8, 9, 10, 11, 12, 13, 14, 15, 17, 18, 19, 20.
8	3	Consumer 1: 10, 11, 12, 13, 14, 15, 16, 17, 18, 19, 20 , 21, (32 kWh); Consumer 2: 1, 2, 3, 6, 7, 8, 9, 10, 11, 12, 13, 14, 15, 17, 18, 19, 20; Consumer 3: 1, 3, 4, 6, 7, 9, 10 11, 12, 13, 15, 16, 17, 18, 19, 20, 21 (20 kWh).
Communities with individual SB		
Community	Number of consumers *u*	Home appliances and EVs *a*
9	3	Consumer 1: 1, 2, 3, 4, 5, 6, 7, 8, 9, 10, 11, 12, 13, 14, 15, 16, 17, 18, 19, 20, 21 (20 kWh); Consumer 2: 1, 2, 3, 4, 5, 6, 7, 8, 9, 10, 11, 12, 13, 14, 15, 16, 17, 18, 19, 20; Consumer 3: 1, 2, 3, 4, 5, 6, 7, 8, 9, 10, 11, 12, 13, 14, 15, 16, 17, 18, 19, 20, 21 (32 kWh).
10	3	
11	4	Consumer 1: 1, 2, 3, 4, 5, 6, 7, 8, 9, 10, 11, 12, 13, 14, 15, 16, 17, 18, 19, 20, 21 (20 kWh); Consumer 2: 1, 2, 3, 4, 5, 6, 7, 8, 9, 10, 11, 12, 13, 14, 15, 16, 17, 18, 19, 20;
12	4	

		Consumer 3: 1, 2, 3, 4, 5, 6, 7, 8, 9, 10, 11, 12, 13, 14, 15, 16, 17, 18, 19, 20, 21 (32 kWh); Consumer 4: 1, 2, 3, 4, 5, 6, 7, 8, 9, 10, 11, 12, 13, 14, 15, 16, 17, 18, 19, 20.
13	3	Consumer 1: 1, 2, 3, 4, 5, 6, 7, 8, 9, 10, 11, 12, 13, 14, 15, 16, 17, 18, 19, 20, 21 (20 kWh); Consumer 2: 1, 2, 3, 4, 5, 6, 7, 8, 9, 10, 11, 12, 13, 14, 15, 16, 17, 18, 19, 20;
14	3	Consumer 3: 1, 2, 3, 4, 5, 6, 7, 8, 9, 10, 11, 12, 13, 14, 15, 16, 17, 18, 19, 20, 21 (32 kWh).

Table 10. SB capacity present in each community

Shared SB			
Capacity community (kWh)	Value	Capacity community (kWh)	Value
$\mathcal{B}^{c1}$	10.0	$\mathcal{B}^{c5}$	10.0
$\mathcal{B}^{c2}$	15.0	$\mathcal{B}^{c6}$	10.0
$\mathcal{B}^{c3}$	10.0	$\mathcal{B}^{c7}$	15.0
$\mathcal{B}^{c4}$	12.0	$\mathcal{B}^{c8}$	12.0
Individual SBs			
Capacity (kWh)	Value per consumer	Capacity (kWh)	Value per consumer
$\mathcal{B}_u^{c9}$	Consumer 1: 5.0 Consumer 2: 6.0 Consumer 3: 4.0	$\mathcal{B}_u^{c12}$	Consumer 1: 4.0 Consumer 2: 8.0 Consumer 3: 4.0 Consumer 4: 6.0
$\mathcal{B}_u^{c10}$	Consumer 1: 6.0 Consumer 2: 8.0 Consumer 3: 4.0	$\mathcal{B}_u^{c13}$	Consumer 1: 8.0 Consumer 2: 5.0 Consumer 3: 5.0
$\mathcal{B}_u^{c11}$	Consumer 1: 8.0 Consumer 2: 6.0 Consumer 3: 8.0 Consumer 4: 6.0	$\mathcal{B}_u^{c14}$	Consumer 1: 5.0 Consumer 2: 5.0 Consumer 3: 5.0

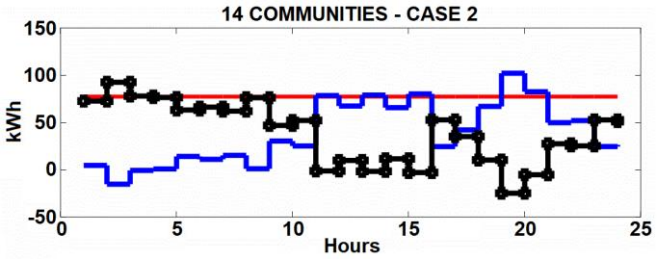

Figure 16. Values related to P_t^{eg} (red) and its components associated with communities with shared SBs (blue) and individual SBs (black).

Fig. 16 shows, in red, power delivered from the PG to the 14 communities, P_t^{eg}. Note that, during the day, P_t^{eg} remains almost constant at around 77.42 kW. In addition, P_t^{eg} does not present peaks in demand, which contributes to relieving PG's operational stress. Still, in Fig. 16, the total power required/supplied by communities supported with shared and individual SBs are presented in blue and black, respectively. Thus, the total power required/supplied by communities supported by shared SBs results from the sum of $P_t^{eg\_c1}$, $P_t^{eg\_c2}$, $P_t^{eg\_c3}$, $P_t^{eg\_c4}$, $P_t^{eg\_c5}$, $P_t^{eg\_c6}$, $P_t^{eg\_c7}$, and $P_t^{eg\_c8}$. For communities with individual SBs, the sum of $P_t^{eg\_c9}$, $P_t^{eg\_c10}$, $P_t^{eg\_c11}$, $P_t^{eg\_c12}$, $P_t^{eg\_c13}$, and $P_t^{eg\_c14}$ represents this total required/supplied power. When the total power is positive in a given period *t*, it indicates that these communities are requesting power. Otherwise, communities are providing power. In the latter case, the supplied power contributes to supporting other communities without influencing the flow direction of P_t^{eg}, as explained in Fig. 4. It is worth mentioning that the power provided by the communities (i.e., with shared SBs or with individual SBs) contributes to the support of the other remaining communities. Based on this, the total power in the blue line shows that communities supported with shared SBs provide powers of 15.15 kW and 0.61 kW during the consecutive periods of 1h – 2h and 2h – 3h, respectively. For the rest of the periods *t*, these communities request power that can come from PG or communities supported with individual SBs, or both.

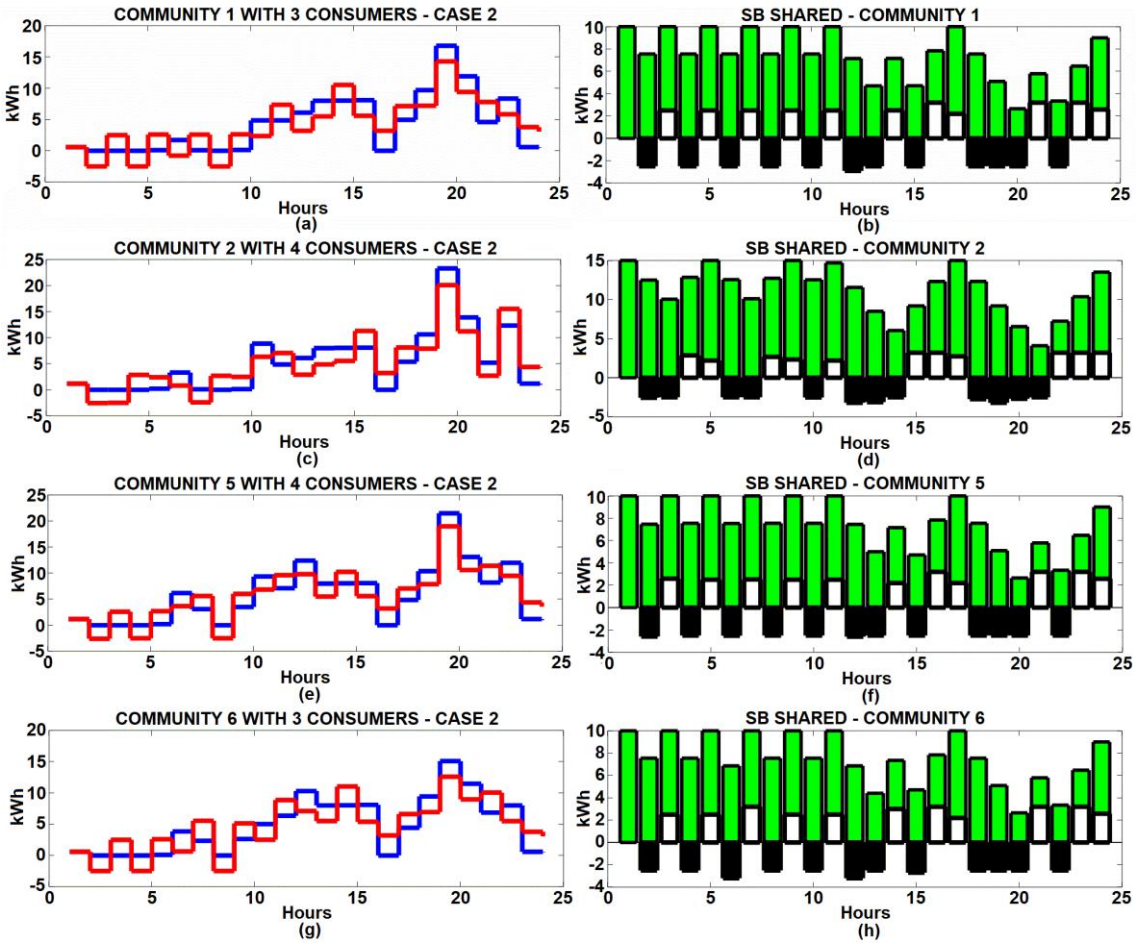

Figure 17. The total habitual profile (blue), power required/supplied (red), SOC (green), power absorbed (white), and power injected (block) related to *Communities 1*, *2*, *5*, and *6*.

In order to show the performance of communities supported with shared SBs, representative *Communities 1*, *2*, *5*, and *6* are used. Thus, Figs. 17 (a), (c), (e), and (g) depict in red and blue the power required/supplied, as well as the habitual profile of total consumption of each of these communities, respectively. It is worth mentioning that this total habitual profile of each community is obtained by the sum of the habitual profiles of all consumers in that community. For example, for *Community 5* with 4 consumers, the power required/supplied by this community is $P_t^{eg\_c5}$ and the total habitual profile results $\mathcal{C}_t^{c5} = \sum_{\forall a \in A} \mathcal{C}_{1,a,t}^{c5} + \sum_{\forall a \in A} \mathcal{C}_{2,a,t}^{c5} + \sum_{\forall a \in A} \mathcal{C}_{3,a,t}^{c5} + \sum_{\forall a \in A} \mathcal{C}_{4,a,t}^{c5}$. Note that during the day, *Communities 1*, *2*, *5*, and *6* provide powers (negative values in red) $P_t^{inj\_c1}$ of 2.50 kW (1h – 2h), 2.5 kW (3h – 4h), 0.78 kW (5h – 6h), 2.50 kW (7h – 8h); $P_t^{inj\_c2}$ of 2.56 kW (1h – 2h), 2.50 kW (2h – 3h), 2.41 kW (6h – 7h); $P_t^{inj\_c5}$ of 2.59 kW (1h – 2h), 2.50 kW (3h – 4h), 2.50 kW (7h – 8h); and $P_t^{inj\_c6}$ of 2.50 kW (1h – 2h), 2.50 kW (3h – 4h), 2.5 kW (7h – 8h), in periods *t* prior to the period 9h – 10h. For periods *t* after the period 9h – 10h, positive values in red related to $P_t^{inj\_c1}$, $P_t^{inj\_c2}$, $P_t^{inj\_c5}$, and $P_t^{inj\_c6}$ indicate that each community is requesting power. Thus, this requested power may be provided by the PG or communities supported by individual SBs, or both.

Figs. 17 (b), (d), (f), and (h) depict, in green bars, the SOC related to shared SBs present in *Communities 1*, *2*, *5*, and *6*. Also, the bars in black (negative values) and white (positive values) represent the injection and absorption powers of each shared SB, in each period *t*, respectively. Considering the previous example, the SOC and injection/absorption power related to *Community 5* are $\mathcal{E}_t^{c5}$, $P_t^{inj\_c5}$, and $P_t^{abs\_c5}$. Note that at the beginning of the day, the SOC of the shared SBs, $\mathcal{E}_t^{c1}$, $\mathcal{E}_t^{c2}$, $\mathcal{E}_t^{c5}$, and $\mathcal{E}_t^{c6}$, reach their total capacity B_t^{c1} = 10 kWh, B_t^{c2} = 15 kWh, B_t^{c5} = 10 kWh, and B_t^{c6} = 10 kWh. In addition, in most periods of the day, the SOC of these SBs adopts values above 50% of the respective capacity. Note also that the lowest SOC values occur in the peak period as well as in periods *t* close to it. Thus, for *Communities 1*, *4*, and *6*, the lowest SOC values of 2.65 kWh and 3.34 kWh occur in periods 19h – 20h and 21h – 22h, respectively. For *Community 2*, the lowest SOC of 4.09 kWh occurs in period 20h – 21h. It is worth mentioning that, during the peak period, the power injection of the shared SBs supports the power supplied by the PG to meet the energy needs of the total number of consumers present in a given community. For example, in *Community 1*, in the period 20h – 21h, the total power requested by the 3 consumers is 11.91 kW. In the same period, the $P_t^{eg\_c1}$ power is supplied with a value of 9.41 kW (red line), while the SB injects a power of 2.50 kW (black bar), thus meeting the energy requirements of these consumers. Therefore, these results show the efficient performance of shared SBs to alleviate the energy supply from the PG in periods of higher stress.

In addition, the performance of communities supported by individual SBs is also analyzed. For this purpose, representative *Communities 9* and *11* are used. It is worth mentioning that, due to these communities having a higher number of appliances (including EVs), a scheduling scheme in the times of usage of home appliances and EV battery charging based on an hourly rate is applied. In this way, based on the habitual consumption profile, an optimal consumption profile is obtained to guarantee the reduction of the electricity bill costs.

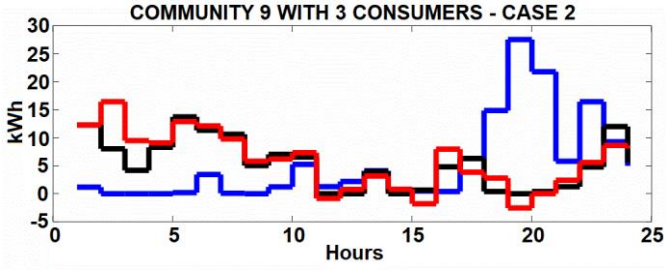

Figure 18. The total habitual profile (blue), the total optimal profile (black), and power required/supplied (red) related to *Community 9*.

Fig. 18 depicts for each period *t* the values of the total habitual profile ($\mathcal{C}_t^{c9} = \sum_{\forall a \in A} \mathcal{C}_{1,a,t}^{c9} + \sum_{\forall a \in A} \mathcal{C}_{2,a,t}^{c9} + \sum_{\forall a \in A} \mathcal{C}_{3,a,t}^{c9}$), the total optimal profile ($\mathcal{O}_t^{c9} = \sum_{\forall a \in A} \mathcal{O}_{1,a,t}^{c9} + \sum_{\forall a \in A} \mathcal{O}_{2,a,t}^{c9} + \sum_{\forall a \in A} \mathcal{O}_{3,a,t}^{c9}$), as well as the power required/supplied, $P_t^{eg\_c9}$, by *Community 9* in blue, black, and red lines, respectively. In the habitual profile, *Community 9* reaches the maximum consumption

of 14.86 kWh, 27.54 kWh, 21.79 kWh, and 16.43 kWh within the intermediate and peak periods. By applying domestic demand scheduling, including EVs demand, the optimal profile obtained for this community presents maximum consumptions of 13.73 kWh, 11.33 kWh, 10.62 kWh, and 12.0 kWh in off-peak periods such as 4h – 5h, 5h – 6h, 6h – 7h, and 22h – 23h, respectively. Notice how the $P_t^{eg\_c9}$ power tries to meet the optimal profile in each period *t*. Thus, in the periods when $P_t^{eg\_c9}$ is greater than $\mathcal{O}_t^{c9}$ (e.g., for periods of 1h – 2h, 2h – 3h, and 15h – 16h), this excess energy is stored in the SBs. Otherwise, when $P_t^{eg\_c9}$ is less than the power request $\mathcal{O}_t^{c9}$ (e.g., 8h – 9h, 12h – 13h, 16h – 17h, and 22h – 23h), then the energy is filled by the individual SBs related to the 3 consumers in this community.

In order to analyze the operational performance of each consumer present in *Community 9*, Figs. 19 (a), (c), and (e) depict the values of the powers $P_{1,t}^{s\_c9}$, $P_{2,t}^{s\_c9}$, and $P_{3,t}^{s\_c9}$ (in red) and $P_{1,t}^{h\_c9}$, $P_{2,t}^{h\_c9}$, and $P_{3,t}^{h\_c9}$ (in blue) related to consumers *u* 1, 2, and 3 for each period *t*. The $P_{u,t}^{h\_c9}$ values correspond to the total power that supplies the home appliances (including or not charging the EV) of the consumer *u* used in period *t*. Due to the domestic demand scheduling strategy (i.e., $\mathcal{O}_{u,a,t}^{c9}$ obtained from $\mathcal{C}_{u,a,t}^{c9}$), $P_{u,t}^{h\_c9}$ meets the $\mathcal{O}_{u,a,t}^{c9}$ profile. Figs. 19 (b), (d), and (f) show the operating regime of each SB belonging to each consumer. In this figure, the green bars indicate the SOC of the individual SB, $\mathcal{E}_{1,t}^{c9}$, $\mathcal{E}_{2,t}^{c9}$, and $\mathcal{E}_{3,t}^{c9}$. The values of the powers of absorption ($P_{1,t}^{abs\_c9}$, $P_{2,t}^{abs\_c9}$, and $P_{3,t}^{abs\_c9}$) and injection ($P_{1,t}^{inj\_9}$, $P_{2,t}^{inj\_c9}$, and $P_{3,t}^{inj\_c9}$) during the day are represented by the respective white and black bars.

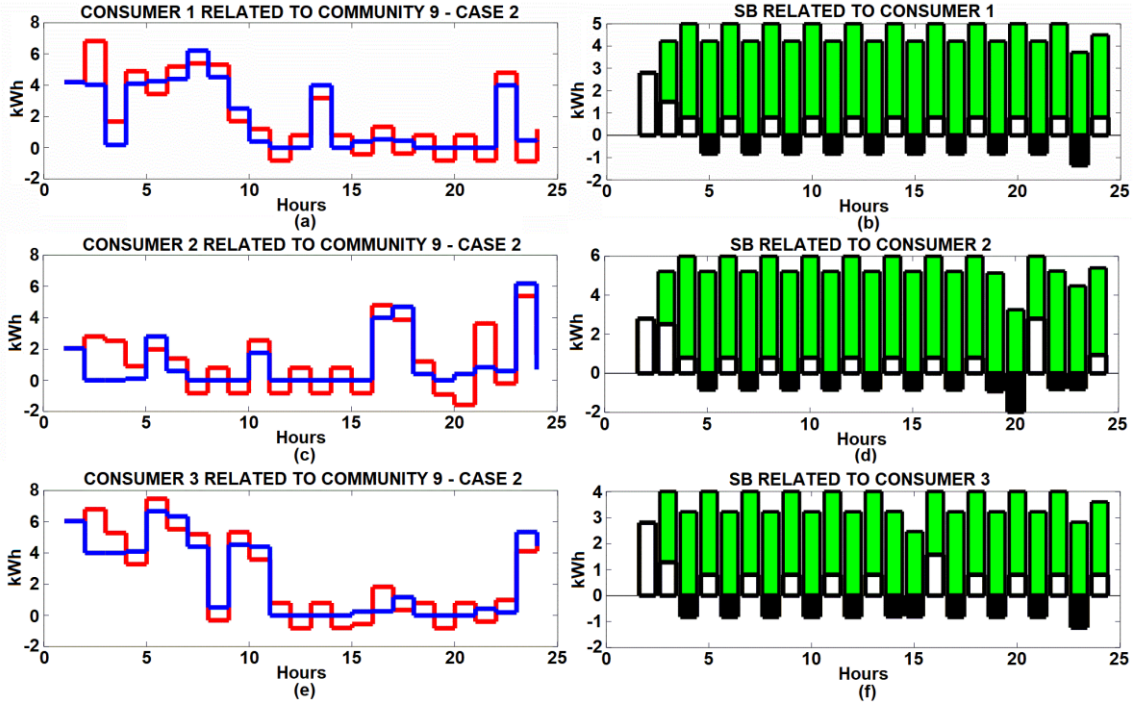

Figure 19. Values of $P_{u,t}^{s\_c9}$ (red), $P_{u,t}^{h\_c9}$ (blue), $\mathcal{E}_{u,t}^{c9}$ (green), $P_{u,t}^{abs\_c9}$ (white), and $P_{u,t}^{inj\_c9}$ (black) for each consumer *u* in the *Community 9*.

Still, in Fig. 19, because the individual SBs start their operation completely uncharged, $\mathcal{E}_{u,t}^{c9} = 0$, at the beginning of the day, period 0h – 1h, the power $P_{u,t}^{s\_c9}$ completely meets the requirements of $P_{u,t}^{h\_c9}$ for all consumers u. After this period, in the two consecutive periods of 1h – 2h and 2h – 3h, the values of $P_{u,t}^{s\_c9}$ (6.83 kW and 1.68 kW for consumer 1; 2.80 kW and 2.52 kW for consumer 2; and 6.80 kW and 5.28 kW for consumer 3, respectively) are higher than $P_{u,t}^{h\_c9}$ (4.03 kW and 0.18 kW for consumer 1; 0.00 kW and 0.00 kW for consumer 2; and 4.0 kW and 4.0 kW for consumer 3, respectively). In this case, part of the power $P_{u,t}^{s\_c9}$ is absorbed by the SBs related to consumer 1 (2.80 kW and 1.50 kW), 2 (2.80 kW and 2.52 kW), and 3 (2.80 kW and 1.28 kW) to be used later. This fact shows that in periods when $P_{u,t}^{s\_c9}$ is greater than $P_{u,t}^{h\_c9}$, the SB stores part of this energy coming from the PG or from the SBs of the community itself or other communities. As a complement, in the periods when $P_{u,t}^{h\_c9}$ is greater than $P_{u,t}^{s\_c9}$, i.e., the power supplied $P_{u,t}^{s\_c9}$ to the consumer u is insufficient. Therefore, the individual SBs inject power to support the requirements of $P_{u,t}^{h\_c9}$.

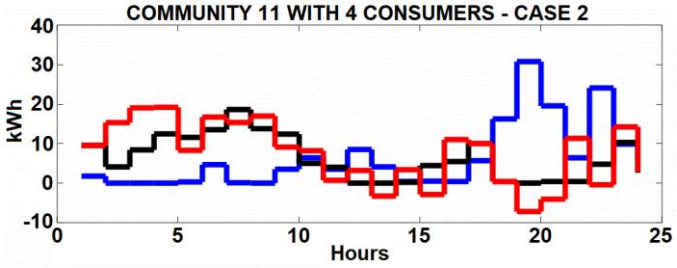

Figure 20. The total habitual profile (blue), the total optimal profile (black), and power required/supplied (red) related to *Community 11*.

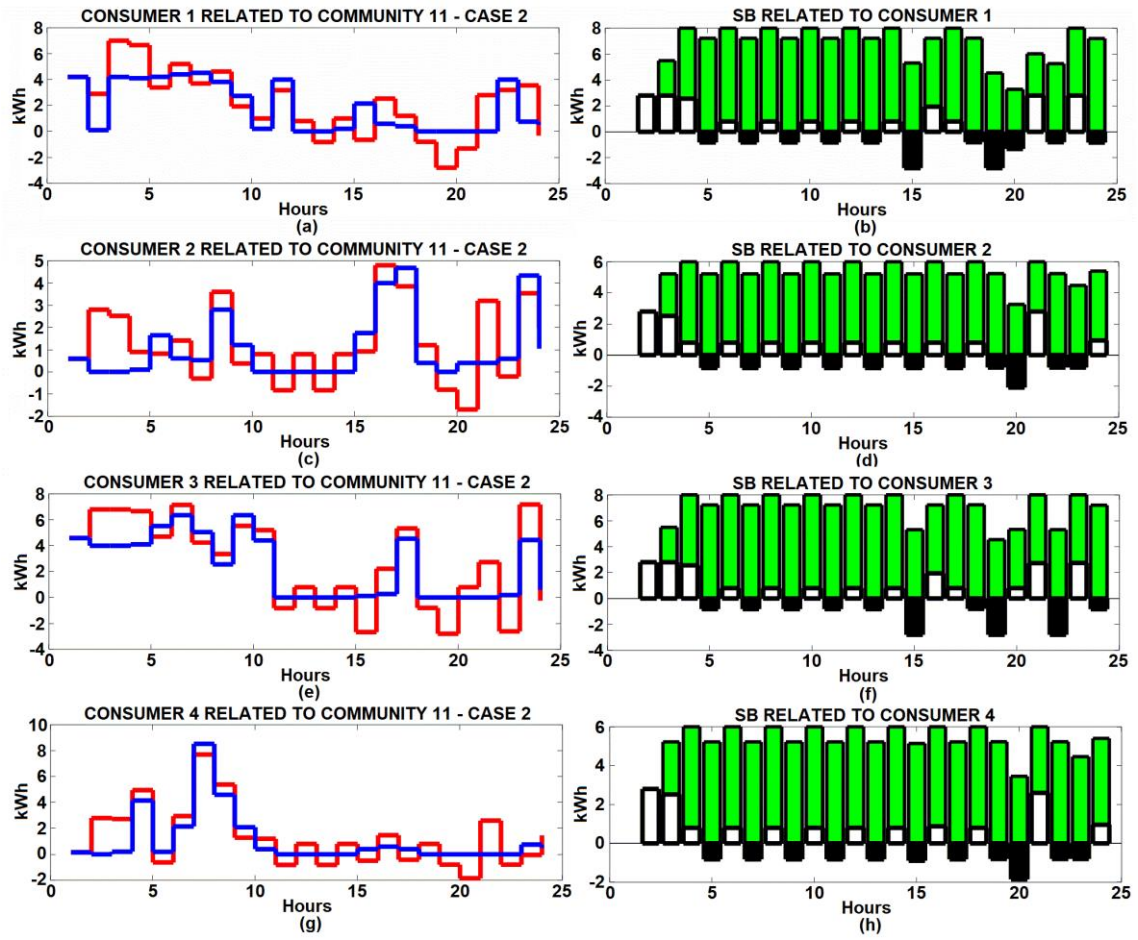

Figure 21. Values of $P_{u,t}^{s\_c11}$ (red), $P_{u,t}^{h\_c11}$ (blue), $\mathcal{E}_{u,t}^{c11}$ (green), $P_{u,t}^{abs\_c11}$ (white), and $P_{u,t}^{inj\_c11}$ (black) for each consumer *u* in the *Community 11*.

Another example related to the performance of a community supported by individual SBs is shown in Figs. 20 and 21. For *Community 11*, Fig. 20 depicts the total profile related to habitual consumption (blue) and optimal consumption (black). This last profile is obtained by applying the scheduling of appliances and charging the EVs associated with the 4 consumers in this community. Note that in the optimal profile, in most periods *t* during the day, the power $P_{u,t}^{s\_c11}$ can meet the consumption requirements of this profile and the storage requirements of $\mathcal{E}_{u,t}^{c11}$, i.e., $P_{u,t}^{s\_c11}$ is greater than $P_{u,t}^{h\_c11}$. Also, for this community, there are a few periods *t* of the day when $P_{u,t}^{s\_c11}$ is insufficient, requiring the injection of power from the SBs. In addition, Fig. 21 shows in detail the values of $P_{u,t}^{s\_c11}$ and $P_{u,t}^{h\_c11}$ during the day, as well as SOC, $\mathcal{E}_{u,t}^{c11}$, and the injection, $P_{u,t}^{inj\_c11}$, and absorption, $P_{u,t}^{abs\_c11}$, powers of the individual SBs related to each consumer *u*. As in *Community 9*, each consumer belonging to *Community 11* also makes efficient use of SB in order to support power $P_{u,t}^{s\_c11}$, especially during intermediate and peak demand periods.

Note that the SBs that support communities have a SOC close to or equal to their respective storage capacities during the day. Therefore, a complete discharge of a given SB does not happen. This fact is corroborated by the average value of the SOC of the SBs during the day,

which turns out to be greater than 50% of the capacity of the respective SB. Thus, for representative *Communities 1*, *2*, *5*, and *6* supported by shared SBs, these average values are 74.7%, 74.6%, 74.8%, and 74.22%, respectively. In addition, the minimum SOC values for each of the above communities correspond to 2.65 kWh (*Community 1*, *5*, and *6* with capacity of 10 kWh) and 4.09 kWh (*Community 2* with a capacity of 15 kWh). For representative communities supported by individual SBs, the average SOC values during the day are 85.8%, 84.8%, and 84% for consumers 1, 2, and 3 of *Community 9*, and 80.4%, 84.7%, 82.5%, and 84.8% for consumers 1, 2, 3, and 4 of *Community 11*, respectively. For *Community 9*, the minimum SOC of the SB related to consumers 1 and 2 is 2.74 kWh, and for consumer 3, the minimum SOC is 2.46 kWh. For all SBs related to *Community 11* consumers, the minimum SOC is over 2.74 kWh. Therefore, the results for a higher number of communities corroborate the efficient operation of the SBs, guaranteeing the optimization of their lifetime, as well as the support of PG to meet the consumption needs of all consumers.

Table 11 shows the total costs related to energy consumption in communities supported by shared and individual SBs. Note that for the 8 communities supported with shared SBs the total consumption turns out to be 307.65$. In the case of the 6 communities supported with individual SBs, the total costs related to habitual consumption reach values close to 300$. This higher value of electricity consumption is because consumers present in *Communities 9*, *10*, *11*, *12*, *13*, and *14* (with individual SBs) have a higher number of appliances compared to consumers 1, 2, 3, 4, 5, 6, 7, and 8 (with shared SBs). Therefore, with the support of the individual SBs, the efficient scheduling of periods for using appliances and charging the EVs' batteries is carried out, obtaining an optimal profile with a total cost that represents 63.7% of the total costs related to the habitual profile of these communities.

Table 11. Electricity consumption costs related to the 14 communities

Communities with shared SB		*Communities with SB individual*		
Communities	Habitual profile Total costs ($)	Communities	Habitual profile total costs ($)	Optimal profile total costs ($)
1, 2, 3, 4, 5, 6, 7, 8	307.65	9, 10, 11, 12, 13, 14	295.87	188.41

5. CONCLUSIONS

In this work, to optimize the operation of small- and large-scale NESCs a MILP model was proposed. For the small-scale NESC (i.e., two communities of consumers), the results have shown how mutual support has contributed to mitigating the occurrence of consumption peaks during the supply from PG. Also, during daily operation, *Community 1*, with shared SB, has contributed together with PG to meet the electricity demands of *Community 2*, especially in off-peak periods when the usage of appliances, as well as the battery charging EVs, are scheduled in

Community 2. At the same time, *Community 2*, with individual SBs, has contributed together with PG to meet the electricity consumption needs of *Community 1* during the peak period. In addition, from both *Cases 1* and *2*, *Case 2* minimizes the number of deep discharges from the SBs and seeks to keep the SOC values close to total capacity, contributing to the optimization of the lifetime.

For large-scale NESC (i.e., fourteen communities of consumers), due to the high presence of SBs (shared and individual), the results show the efficient operation of each SB without reaching full discharge at any period of the day. Therefore, the presence of SBs on a large scale contributes to reducing self-fatigue and PG fatigue (during peak demand and peak rebound), supporting the electricity consumption of the total consumer communities. As the results corroborate, by applying the proposed model, NESCs of different scales achieve monetary savings for the total number of consumers (see Tables 8 and 11). For consumers with a higher number of appliances, financial savings result from reduced consumption at peak hours (due to the scheduling of domestic loads). In addition, demand shifted to off-peak hours is supplied through SBs shared and PG. For communities that do not apply the scheduling of domestic loads, the SBs together with the supply from PG contribute to meeting the peak demand. Therefore, our proposal demonstrates its potential to contribute to the operational relief of the PG during the day through the efficient operational scheme of the NESCs.

As the main advantages of this work, we can highlight that the NESCs a) contribute to reducing the PG congestion that can be caused by the high injection of excess power coming from the RSs; b) assist the distribution network operator through the DR strategy aiming at lowering demand peaks during daily supply, i.e., improving the LF; and c) ensure efficient coordination between SBs from communities with different household incomes, as well as the same household income. Like other models, our proposal also has its disadvantages or limitations which has been observed during the analysis of the results. For example, when the number of low-income consumers is much higher than the high-income consumers, the DR strategy may prove insufficient to lower the peak demand. Also, depending on the capacity of each SB, discharge cycles can occur during the day, leading to premature aging of the SBs.

Given these limitations, our future work focuses on determining the allocation (individual or shared, or both), as well as the sizing of SBs considering the adoption of DR strategies (or not) by each consumer, regardless of the level of household income. And in each approach, PG's operational relief related to mitigating peak electricity consumption will be targeted. Finally, other future research should consider the implementation of off-grid RSs as a complementary source for charging SBs and EV batteries associated with communities with differentiated household income.

REFERENCES

[1] European Parliament. Mapping Smart Cities in the EU 2014. https://www.europarl.europa.eu/RegData/etudes/etudes/join/2014/507480/IPOL-ITRE_ET%282014%29507480_EN.pdf. (Accessed 3 Apr 2021)

[2] European Commission. Energy communities: an overview of energy and social innovation 2020 [Online]. Available: https://op.europa.eu/en/publication-detail/-/publication/a2df89ea-545a-11ea-aece-01aa75ed71a1/language-en (Accessed 2 May 2021).

[3] O'Dwyer E, Pan I, Acha S, Shah N. Smart energy systems for sustainable smart cities: Current developments, trends and future directions. Appl. Energy 2019; 237; 581−597. https://doi.org/10.1016/j.apenergy.2019.01.024.

[4] Visvizi A, Lytras M D. Smart Cities: Issues and Challenges – Mapping Political, Social and Economic Risks and Threats. 2019. Elsevier Inc.

[5] Ceglia F, Esposito P, Marrasso E, Sasso M. From smart energy community to smart energy municipalities: Literature review, agendas and pathways. J. Clean. Prod. 2020; 254; 120118. https://doi.org/10.1016/j.jclepro.2020.120118.

[6] Hoang A T, Pham V V, Nguyen X P. Integrating renewable sources into energy system for smart city as a sagacious strategy towards clean and sustainable process. J. Clean. Prod. 2021; 305; 127161. https://doi.org/10.1016/j.jclepro.2021.127161.

[7] Ekanayake J, Liyanage K, Wu J, Yokoyama A, Jenkins N. Smart grid technology and applications 2012. UK: John Wiley & Sons.

[8] Sioshansi F P. Smart grid integrating renewable, distributed & efficiency energy 2012. Elsevier Inc.

[9] Shakouri G, Kazemi A. Multi-objective cost-load optimization for demand side management of a residential area in smart grids. Sustain. Cities Soc. 2017; 32, 171–180. https://doi.org/10.1016/j.scs.2017.03.018.

[10] Dongol D, Feldmann T, Schmidt M, Bollin E. A model predictive control based peak shaving application of battery for a household with photovoltaic system in a rural distribution grid. Sustain. Energy Grids Netw. 2018; 16; 1–13. https://doi.org/10.1016/j.segan.2018.05.001.

[11] Zhou S, Zou F, Wu Z, Gu W, Hong Q, Booth C. A smart community energy management scheme considering user dominated demand side response and P2P trading. Int. J. Electr. Power Energy Syst. 2020; 114; 105378. https://doi.org/10.1016/j.ijepes.2019.105378.

[12] Xing X, Xie L, Meng H. Cooperative energy management optimization based on distributed MPC in grid-connected microgrids community. Int. J. Electr. Power Energy Syst. 2019; 107; 186–199. https://doi.org/10.1016/j.ijepes.2018.11.027.

[13] Ponce-Jara M A, Ruiz E, Gil R, Sancristóbal E, Pérez-Molina C, Castro M. Smart Grid: Assessment of the past and present in developed and developing countries. Energy Strategy Rev., 2017; 18; 38–52. https://doi.org/10.1016/j.esr.2017.09.011.

[14] Marah R, El Hibaoui A. Algorithms for Smart Grid management. Sustain. Cities Soc. 2018; 38; 627–635. https://doi.org/10.1016/j.scs.2018.01.041.

[15] Nuchprayoon S. Calculation and allocation of load losses in distribution system using load research data and load factor method. In: 6th IEEE International Conference on Control System, Computing and Engineering, ICCSCE 2016, IEEE; 2016, p. 85−90. https://doi.org/10.1109/ICCSCE.2016.7893550.

[16] Cerna F V, Contreras J. A MILP model to relieve the occurrence of new demand peaks by improving the load factor in smart homes. Sustain. Cities Soc. 2021; 71; 102969. https://doi.org/10.1016/j.scs.2021.102969.

[17] Singh P, Dhundhara S, Verma Y P, Tayal N. Optimal battery utilization for energy management and load scheduling in smart residence under demand response scheme. Sustain. Energy, Grids Netw. 2021; 26; 100432. https://doi.org/10.1016/j.segan.2021.100432.

[18] Hossain M A, Chakrabortty R K, Ryan M J, Pota H R. Energy management of community energy storage in grid-connected microgrid under uncertain real-time prices. Sustain. Cities Soc. 2021; 66; 102658. https://doi.org/10.1016/j.scs.2020.102658.

[19] Fernandez E, Hossain M J, Mahmud K, Nizami M S H, Kashif M. A Bi-level optimization-based community energy management system for optimal energy sharing and trading among peers. J. Clean. Prod. 2021; 279; 123254. https://doi.org/10.1016/j.jclepro.2020.123254.

[20] Sasidharan N, Singh J G. A resilient DC community grid with real time ancillary services management. Sustain. Cities Soc. 2017; 28; 367–386. https://doi.org/10.1016/j.scs.2016.10.007.

[21] Elkadeem M R, Wang S, Azmy A M, Atiya E G, Ullah Z, Sharshir S W. A systematic decision-making approach for planning and assessment of hybrid renewable energy-based microgrid with techno-economic optimization: A case study on an urban community in Egypt. Sustain. Cities Soc. 2020; 54; 102013. https://doi.org/10.1016/j.scs.2019.102013.

[22] Liang J, Shirsat A, Tang W. Sustainable community based PV-storage planning using the Nash bargaining solution. Int. J. Electr. Power Energy Syst. 2020; 118; 105759. https://doi.org/10.1016/j.ijepes.2019.105759.

[23] Duvignau R, Heinisch V, Goransson L, Gulisano V, Papatriantafilou. Benefits of small-size communities for continuous cost-optimization in peer-to-peer energy sharing. Appl. Energy 2021; 301; 117402. https://doi.org/10.1016/j.apenergy.2021.117402.

[24] Elkazaz M, Summer M, Naghiyev E, Hua Z, Thomas D W P. Techno-Economic Sizing of a community battery to provide community energy billing and additional ancillary services. Sustain. Energy, Grids Netw. 2021; 26; 100439. https://doi.org/10.1016/j.segan.2021.100439.

[25] Liu Y J, Lin C W, Chen S I. Analysis of load electricity consumption on a low-voltage distribution system with community energy storages In: IEEE 3rd International Future Energy Electronics Conference and ECCE Asia, IFEEC – ECCE 2017, IEEE; 2017, p. 2048−2052 https://doi.org/10.1109/IFEEC.2017.7992366.

[26] Lee J O, Kim Y S, Kim T H, Moon S I. Novel droop control of battery energy storage systems based on battery degradation cost in islanded DC microgrids. IEEE Access 2020; 8; 119337–119345. https://doi.org/10.1109/ACCESS.2020.3005158.

[27] Fortenbacher P, Mathieu J L, Andersson G. Modeling and optimal operation of distributed battery storage in low voltage grids. IEEE Trans. Power. Syst. 2017; 32; 4340–4350. https://doi.org/10.1109/TPWRS.2017.2682339.

[28] Moghaddan I N, Chowdhury B H, Mohajeryami S. Predictive operation and optimal sizing of battery energy storage with high wind energy penetration. IEEE Trans. Ind. Electron. 2018; 65; 6686–6695. https://doi.org/10.1109/TIE.2017.2774732.

[29] Weckesser T, Dominkovic D F, Blomgren E M V, Schledorn A, Madsen H. Renewable Energy Communities: Optimal sizing and distribution grid impact of photovoltaics and battery storage. Appl. Energy 2021; 301; 117408. https://doi.org/10.1016/j.apenergy.2021.117408.

[30] Mamounakis I, Efthymiopoulos N, Makris P, Vergados D J, Tsaousoglou G, Varvarigos E. A novel pricing scheme for managing virtual energy communities and promoting behavioral change towards energy efficiency. Electr. Power Syst. Res. 2019; 167; 130–137. https://doi.org/10.1016/j.epsr.2018.10.028.

[31] Anees A, Dillon T, Wallis S, Chen Y P P. Optimization of day-ahead and real-time prices for smart home community. Int. J. Electr. Power Energy Syst. 2021; 124; 106403. https://doi.org/10.1016/j.ijepes.2020.106403.

[32] Cheng P H, Huang T H, Chien Y W, Wu C L, Tai C S, Fu L C. Demand-side management in residential community realizing sharing economy with bidirectional PEV while additionally considering commercial area. Int. J. Electr. Power Energy Syst. 2020; 116; 105512. https://doi.org/10.1016/j.ijepes.2019.105512.

[33] Li P, Wang Z, Wang N, Yang W, Li M, Zhou X, Yin Y, Wang J, Guo T. Stochastic robust optimal operation of community integrated energy system based on integrated demand response. Int. J. Electr. Power Energy Syst. 2021; 128; 106735. https://doi.org/10.1016/j.ijepes.2020.106735.

[34] Cerna F V, Pourakbari-Kasmaei M, Pinheiro L S S, Naderi E, Lehtonen M, Contreras J. Intelligent Energy Management in a Prosumer Community Considering the Load Factor Enhancement. Energies 2021; 14; 3624. https://doi.org/10.3390/en14123624.

[35] Garcia-Villalobos J, Zamora I, Eguia P, Torres E, Etxegarai A, San Martin J I. Optimization of load factor in distribution networks with high share of plug-in electric vehicles and photovoltaic generation. In: 52nd International Universities Power Engineering Conference, UPEC 2017, IEEE; 2017, p. 1−6. https://doi.org/10.1109/UPEC.2017.8231917.

[36] Trongwanichnam K, Thitapars S, Leeprechanon N. Impact of Plug-in Electric Vehicles Load Planning to Load Factor and Total Generation Cost in a Power System. In: IEEE PES GTD Grand International Conference and Exposition Asia, GTD Asia 2019, IEEE; 2019, p. 599−604. https://doi.org/10.1109/GTDAsia.2019.8716008.

[37] Residential Class Brazil Report – Procel/Eletrobrás - 2007. Survey of possession of equipment and habits of use – Base year 2005 [Online]. Available: file:///C:/Users/SAMSUNG/Downloads/Classe_Residencial_Relatorio_Brasil.pdf (Accessed 09 May 2021).

[38] Anzar M, Iqra R, Kousar A, Ejaz S, Alvarez-Alvarado M S, Zafar A K. Optimization of home energy management system in smart grid for effective demand side management. In: International Renewable and Sustainable Energy Conference, IRSEC 2018. IEEE; 2018, p. 1−6. https://doi.org/10.1109/IRSEC.2017.8477255.

[39] Cerna F V, Pourakbari-Kasmaei M, Romero R A, Rider M J. Optimal delivery scheduling and charging of EVs in the navigation of a city map. IEEE Trans Smart Grid 2018; 9; 4815–4827. https://doi.org/10.1109/TSG.2017.2672801.

[40] Robert P C, Casella G. Monte Carlo Statistical Methods. Springer Science+Business Media New York 2004.

[41] Zio E, Delfanti M, Giorgi L, Olivieri V, Sansavini, G. Monte Carlo simulation-based probabilistic assessment of DG penetration in medium voltage distribution networks. Int. J. Electr. Power Energy Syst. 2015; 64; 852–860. https://doi.org/10.1016/j.ijepes.2014.08.004.

[42] Wang Y, Infield D. Markov chain Monte Carlo Simulation of electric vehicles use for network integration studies. Int. J. Electr. Power Energy Syst. 2018; 99; 85–94. https://doi.org/10.1016/j.ijepes.2018.01.008.

[43] US Department of Energy. Appliance & Equipment Standards/Standards and Test Procedures 2019 [Online]. Available: https://www.energy.gov/eere/buildings/standards-and-test-procedures (Accessed 15 Jun 2020).

[44] Chuan L, Ukil A. Modeling and validation of electrical load profiling in residential building in Singapore. IEEE Trans. Power. Syst. 2015; 30; 2800–2809. https://doi.org/10.1109/PESGM.2015.7286345.

[45] Ebrahimi H, Abapour M, Mohammadi-Ivatloo B, Golshannavaz S, Yazdaninejadi A. Decentralized approach for security enhancement of wind-integrated energy systems coordinated with energy storages. Int. J. Energy Res. 2021; 46; 5006 – 5027. https://doi.org/10.1002/er.7494.

[46] Borges M C O, Franco J F, Rider M J. Optimal reconfiguration of electrical distribution systems using mathematical programming. J. Control Autom. Electr. Syst. 2014; 25; 103–111. https://doi.org/10.1007/s40313-013-0070-x.

[47] Cerna F V, Pourakbari-Kasmaei M, Lehtonen M, Contreras J. Efficient automation of an HEV heterogeneous fleet using a two-stage methodology. IEEE Trans. Veh. Technol. 2019; 68; 9494–9506. https://doi.org/10.1109/TVT.2019.2937452.

[48] ANEEL. Normative Resolution 733, 6 September 2016. National Agency of Electrical Energy 2016 [Online]. Available: http://www2.aneel.gov.br/cedoc/ren2016733.pdf (Accessed 15 Jun 2020)

[49] Di Santo K G, Kanashiro E, Di Santo S G, Saidel M A. A review on smart grids and experiences in Brazil. Renew. Sustain. Energy Rev. 2015; 54; 1072–1082. https://doi.org/10.1016/j.rser.2015.07.182.

[50] Fourer R, Gay D M, Kernighan B W. *AMPL: a modeling language for mathematical programming'*. Brooks/Cole-Thomson Learning, Pacific Grove 2003, 2nd Ed.

[51] IBM ILOG CPLEX V 12. 1. *'User's manual for CPLEX'*. CPLEX Division, ILOG Inc., Incline Village 2009, NV, USA.